CHAPTER IV

RESULTS

1. Characterization of pralidoxime chloride starting material

1.1 Morphology study

Pralidoxime chloride powders were examined using scanning electron microscope at different magnifications. The shape and surface of pralidoxime chloride powder is illustrated in Figure 9.

1.2 X-ray powder diffraction analysis

Pralidoxime chloride powder was examined using x-ray powder diffraction analysis. The x-ray powder diffraction pattern is illustrated in Figure 10. The XRPD pattern consists of a series of peaks detected at characteristic scattering angles to be used as reference for the starting material in order to compare with that of the subsequent ones. Pralidoxime chloride starting material powder was indicated by the strong and sharp peak intensities, especially at three main sharp diffraction peaks at 17.5^{o} , 23^{o} and 28^{o} 2θ.

1.3 Thermal analysis study

DSC pattern is illustrated in Figure 11. The onset melting temperature of pralidoxime chloride was at approximately $220^{o}C$ and the peak was located at $224^{o}C$. There were no other thermal events shown from temperatures $25^{o}C$ to $210^{o}C$ on the DSC thermogram.

1.4 Infrared Spectrophotometry

The infrared absorption spectrum of pralidoxime chloride powder is shown in Figure 12. The principle peaks were aromatic compound at wave number around 1500 cm^{-1} and wave number 2700 cm^{-1}.

2. Thermal analysis of pralidoxime chloride frozen solution

2.1 Frozen behavior without thermal treatment

2.1.1 Preliminary freezing study

DSC was used as a tool to freeze 5% pralidoxime chloride solution and as a thermal analytical method to detect a change in thermal behavior of the frozen solution.

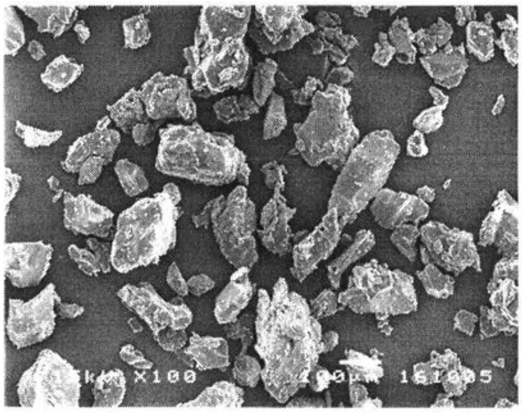

A

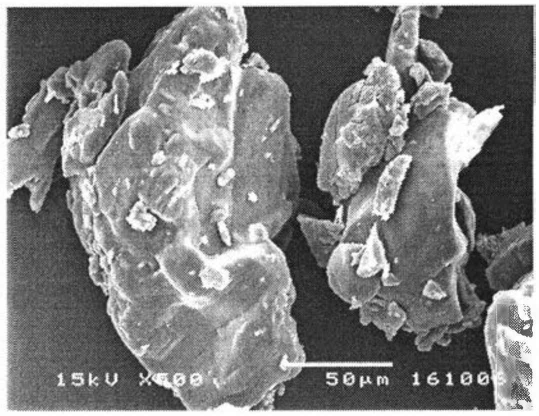

B

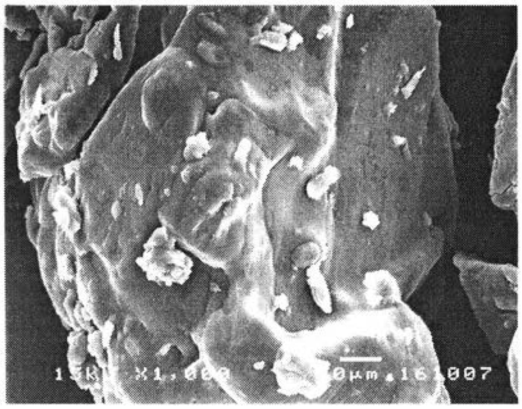

C

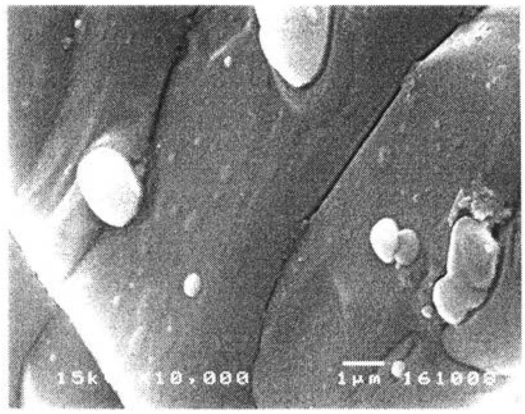

D

Figure 9 Photomicrograph of pralidoxime chloride powder at different magnification

A : x 100, B : x500, C : x1,000 and D : x10,000

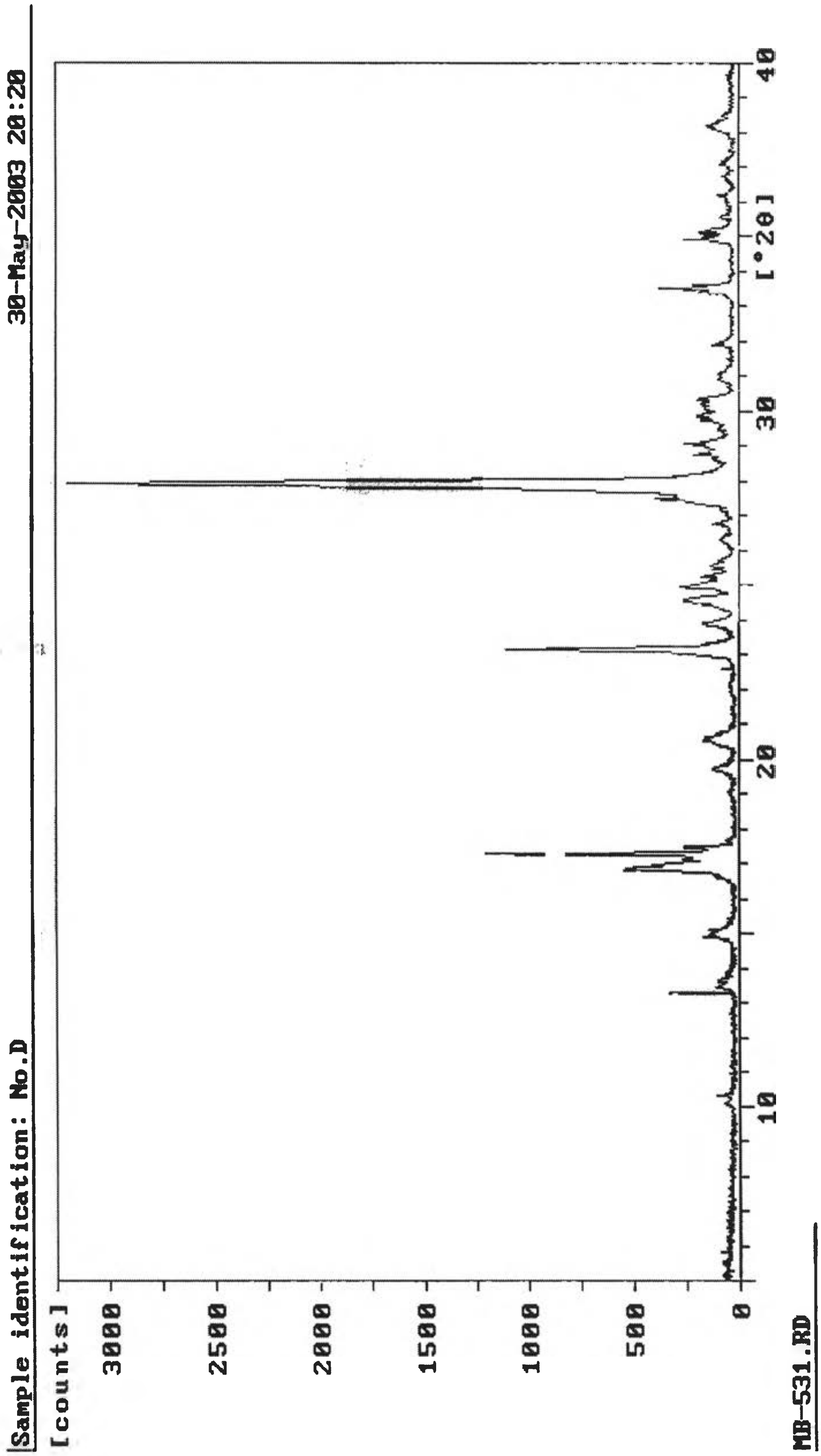

Figure 10 X-ray powder diffractogram of pralidoxime chloride starting material powder.

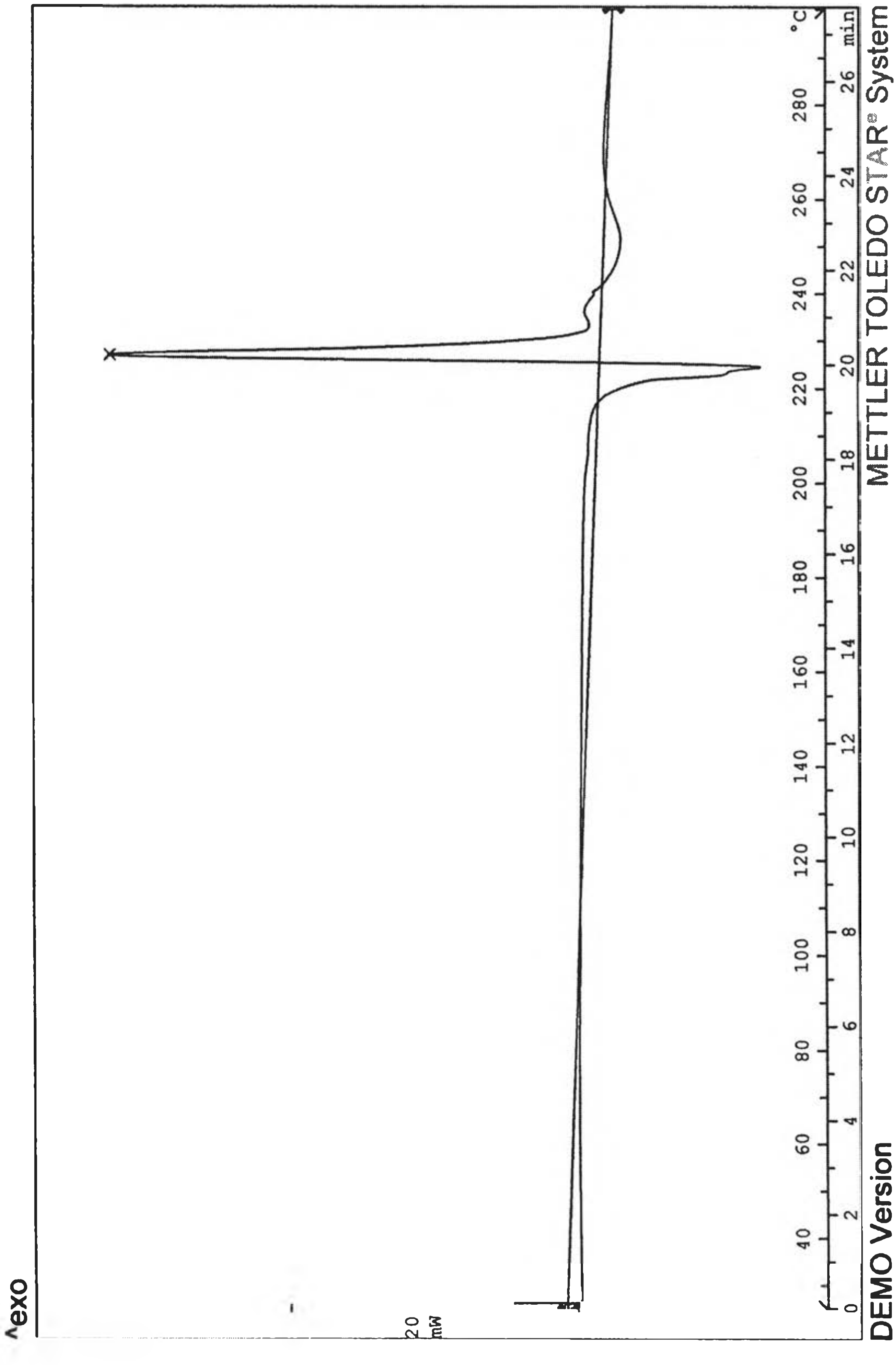

Figure 11 DSC thermogram of pralidoxime chloride starting material powder scanned from $25^{\circ}C$ to $300^{\circ}C$ at a scan rate of $10^{\circ}C/min$.

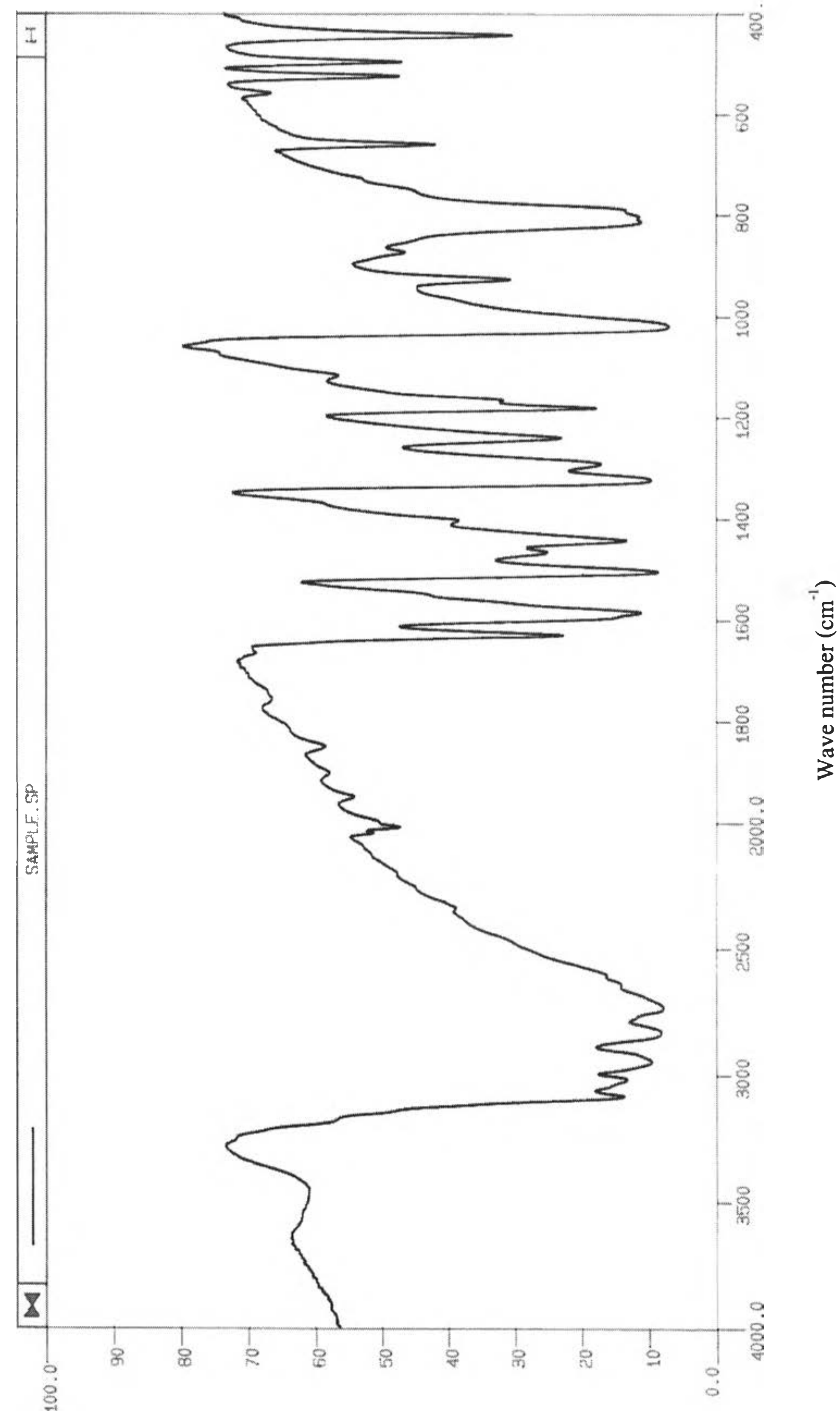

Figure 12 The infrared absorption spectrum of pralidoxime chloride starting material powder.

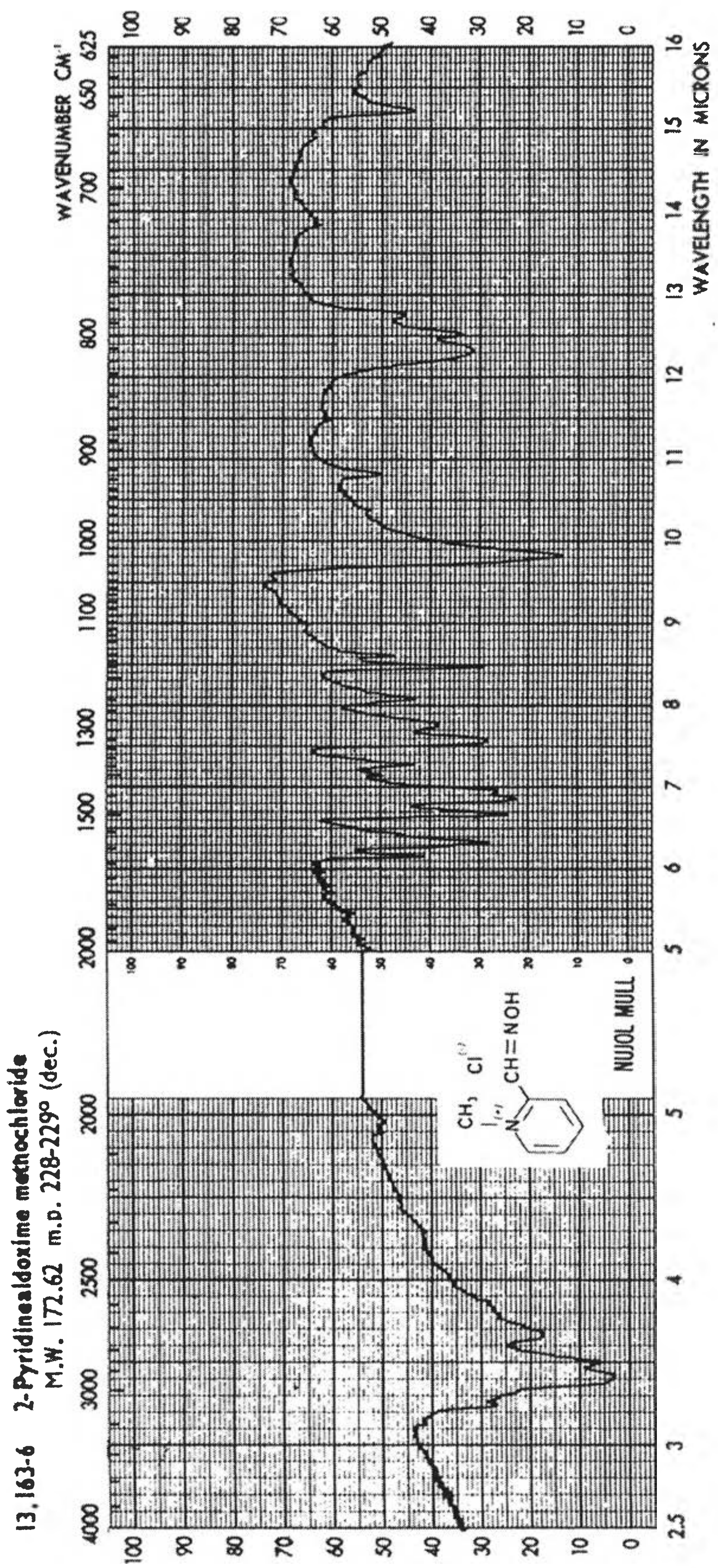

Figure 13 The standard infrared spectrum of pralidoxime chloride from "The Aldrich Library of Infrared Spectrum Ed. III"

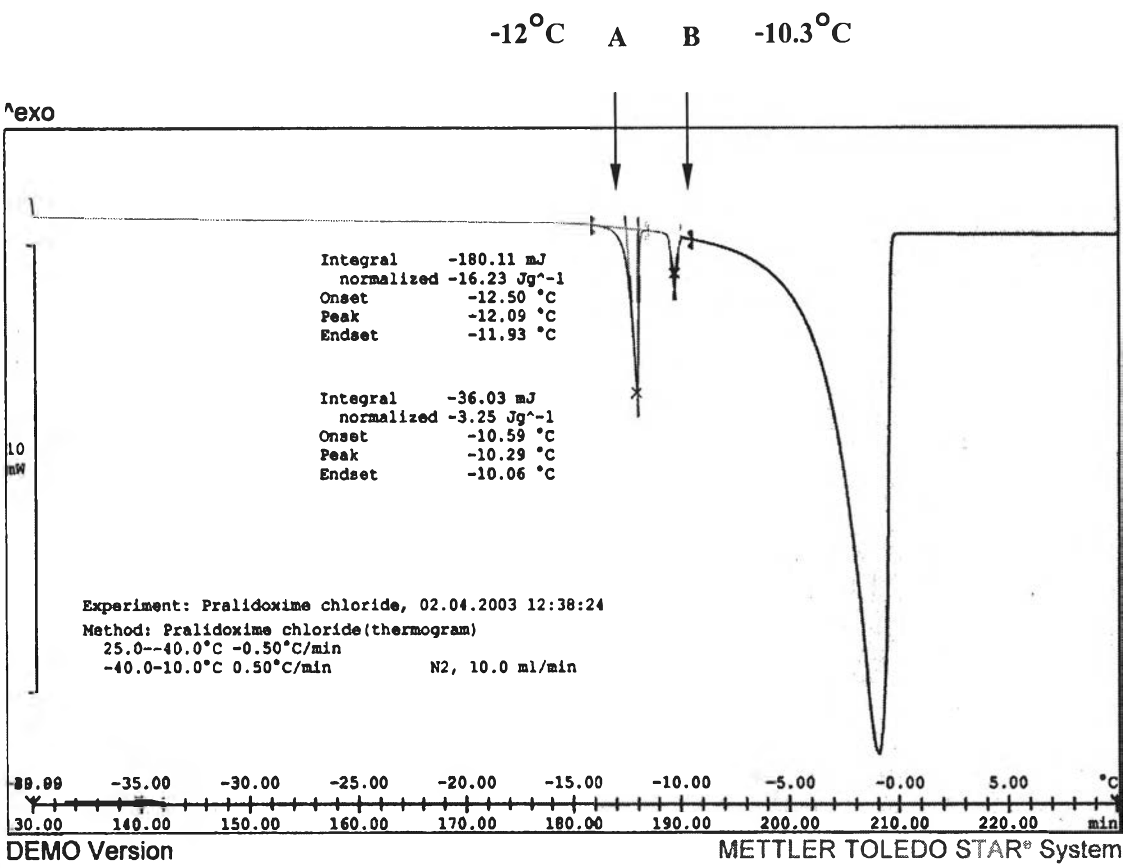

Figure 14 DSC thermogram of 5% pralidoxime chloride solution during heating cycle of 0.5°C/min. (cooling from 25°C to –40°C at the rate of 0.5°C/min.) from temperature 25°C to -40°C and -40°C to 10°C.

The sample was cooled at $0.5^{\circ}C/min$ from $25^{\circ}C$ to $-40^{\circ}C$ followed by heating from $-40^{\circ}C$ to $10^{\circ}C$ at $0.5^{\circ}C/min$. The DSC thermograms are shown in Figure 14.

When pralidoxime chloride was frozen, an exotherm with an onset at $-20^{\circ}C$ was observed (data not shown). During heating, there were no thermal events between -40 to $-20^{\circ}C$. Three endotherms were found in DSC thermogram at eutectic melting region. The temperatures of three endotherms are $-12^{\circ}C$ (peak A) and $-10.3^{\circ}C$ (peak B) and $0^{\circ}C$ (peak C), respectively.

2.1.2 Thermal behavior of frozen solution comparing various cooling rates

Samples were cooled from room temperature ($25^{\circ}C$) to freezing temperature ($-40^{\circ}C$) and heated to $10^{\circ}C$ at different rates. The cooling and heating rates were varied at 1, 5, 10, $20^{\circ}C/min$ as described in Table 2. The DSC thermograms obtained are shown in Figures 15 – 22.

In Figure 15, DSC thermograms of 5% pralidoxime chloride solution were scanned by using the same heating rate at $1^{\circ}C/min$ but different cooling rates of 1,5,10 and $20^{\circ}C/min$. The three endothermic peaks were observed at the temperatures of approximately -12, -10 and $0^{\circ}C$, respectively. The three peaks were located at the same position.

For Figure 16, DSC patterns of pralidoxime chloride solution were scanned by using heating rate of $5^{\circ}C/min$ but different cooling rates. During heating, all thermograms present only two endothermic peaks. The observed endotherms represented at approximately $-11^{\circ}C$ and $2^{\circ}C$.

In Figure 17, the thermal events at melting region show two endothermic peak at approximately $-10^{\circ}C$ and $4^{\circ}C$.

In Figure 18, the heating rate was set at $20^{\circ}C/min$ for every thermograms with various cooling rates. Two endothermic peaks were found at the temperature of approximately $-9^{\circ}C$ and $4^{\circ}C$ with low heat capacity.

2.1.3 Thermal behavior of frozen solution comparing various heating rates

The experiment was set similar to that of experiment 2.2. DSC thermograms were compared when scanned using the same cooling rate but different heating rates.

Table 2 The scanning rates for DSC thermogram at different cooling and heating rate

Figure	Cooling rate	Heating rate	Figure	Heating rate	Cooling rate
15A	1	1	19A	1	1
15B	5	1	19B	5	1
15C	10	1	19C	10	1
15D	20	1	19D	20	1
16A	1	5	20A	1	5
16B	5	5	20B	5	5
16C	10	5	20C	10	5
16D	20	5	20D	20	5
17A	1	10	21A	1	10
17B	5	10	21B	5	10
17C	10	10	21C	10	10
17D	20	10	21D	20	10
18A	1	20	22A	1	20
18B	5	20	22B	5	20
18C	10	20	22C	10	20
18D	20	20	22D	20	20

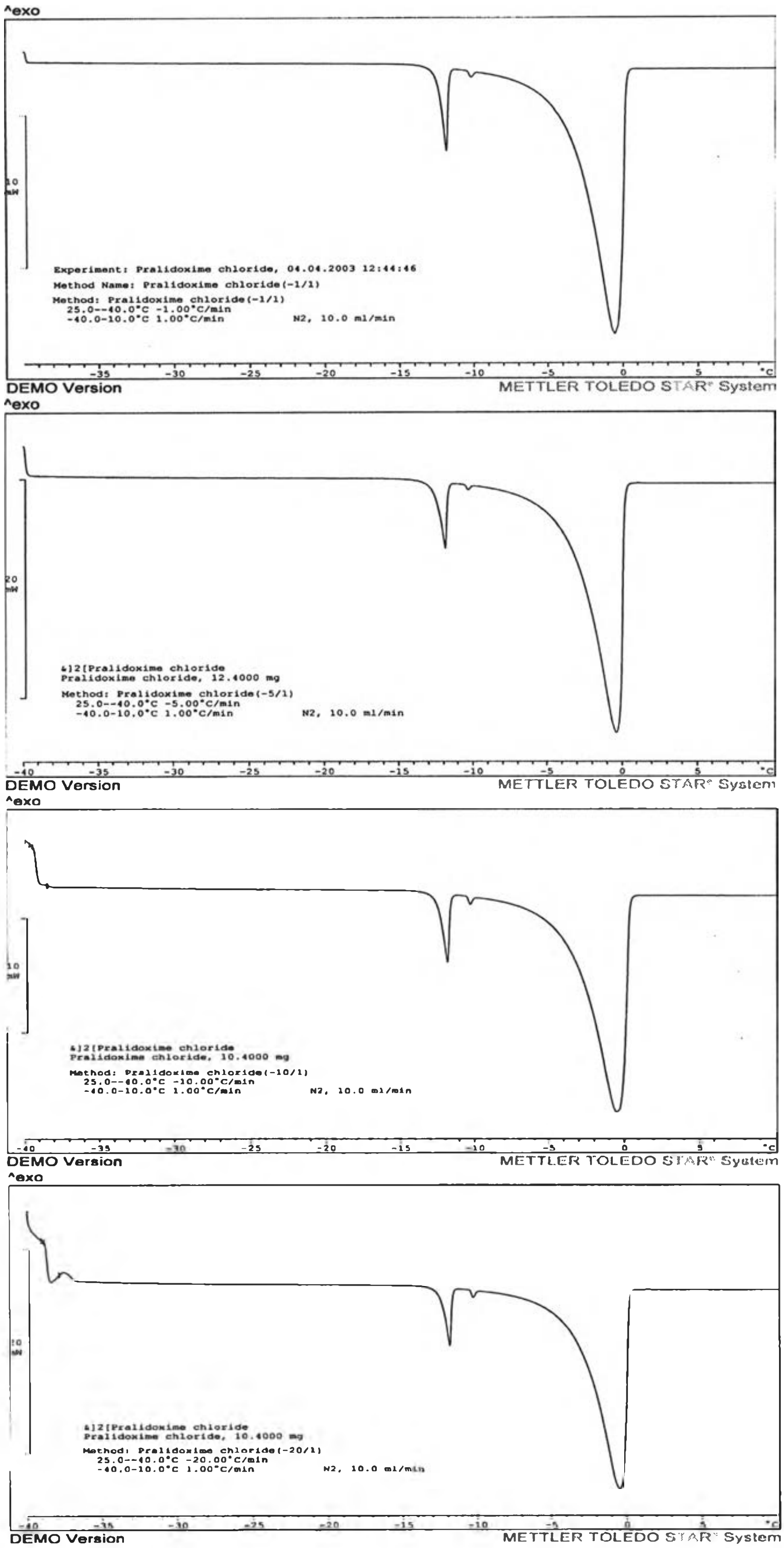

A: Cooling rate = 1 $^{\circ}$C/min.

B: Cooling rate = 5 $^{\circ}$C/min.

C: Cooling rate = 10 $^{\circ}$C/min.

D: Cooling rate = 20 $^{\circ}$C/min.

Figure 15 DSC thermogram with the same heating rate of 1 $^{\circ}$C/min but with various cooling rates

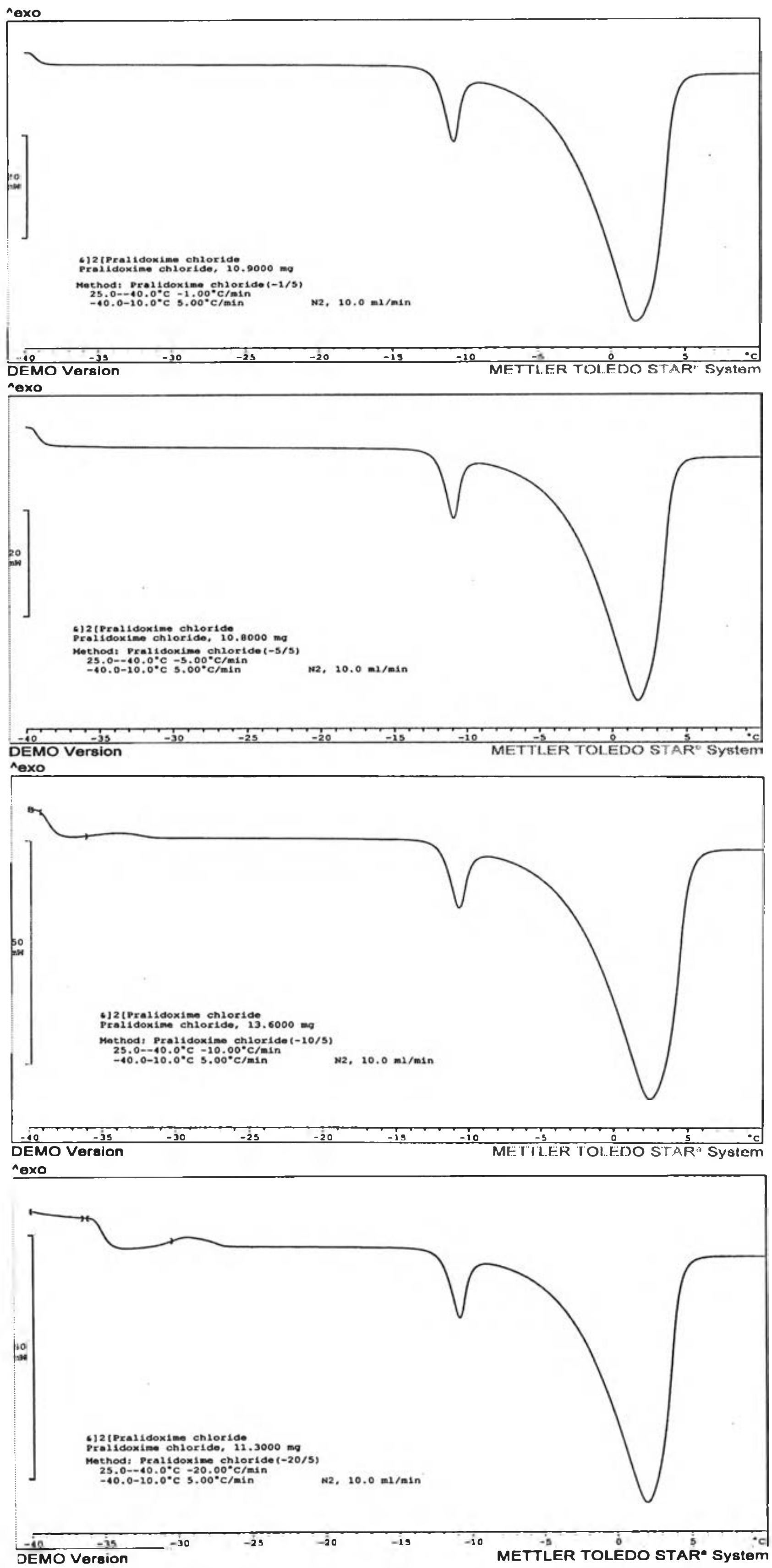

A: Cooling rate = 1°C/min.

B: Cooling rate = 5°C/min.

C: Cooling rate = 10°C/min.

D: Cooling rate = 20°C/min.

Figure 16 DSC thermogram with the same heating rate of 5°C/min but with various cooling rates

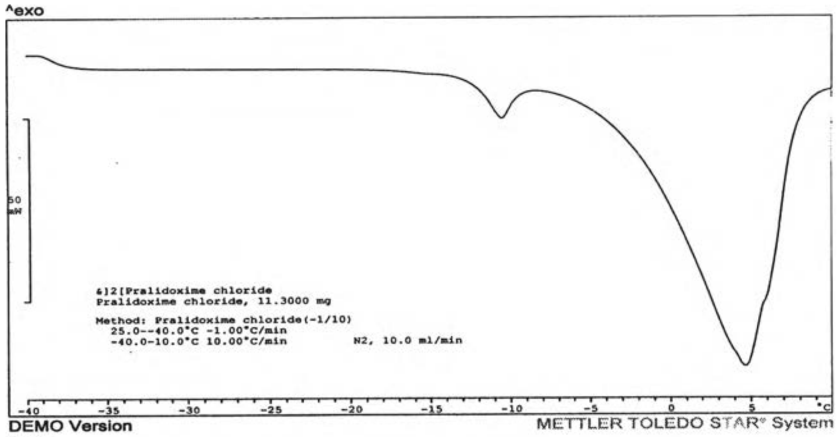

A: Cooling rate = 1°C/min.

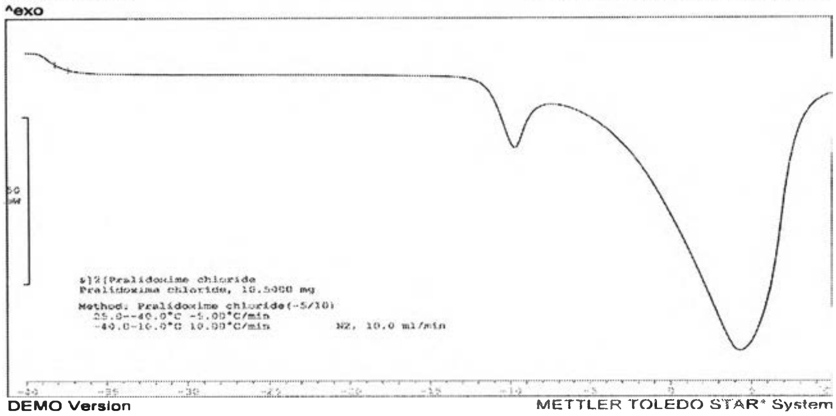

B: Cooling rate = 5°C/min.

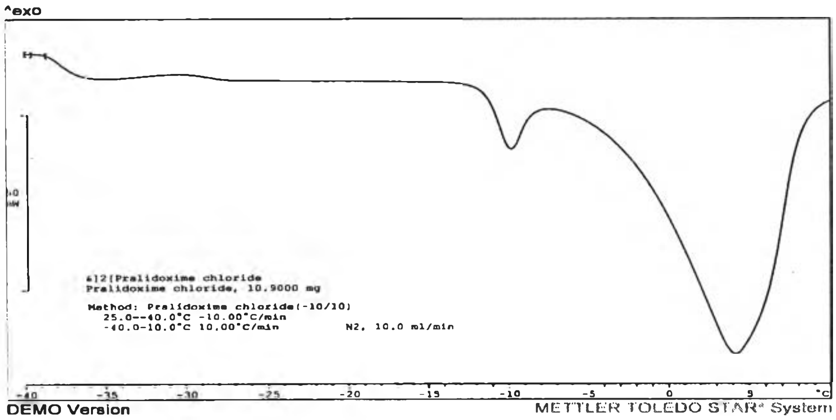

C: Cooling rate = 10°C/min.

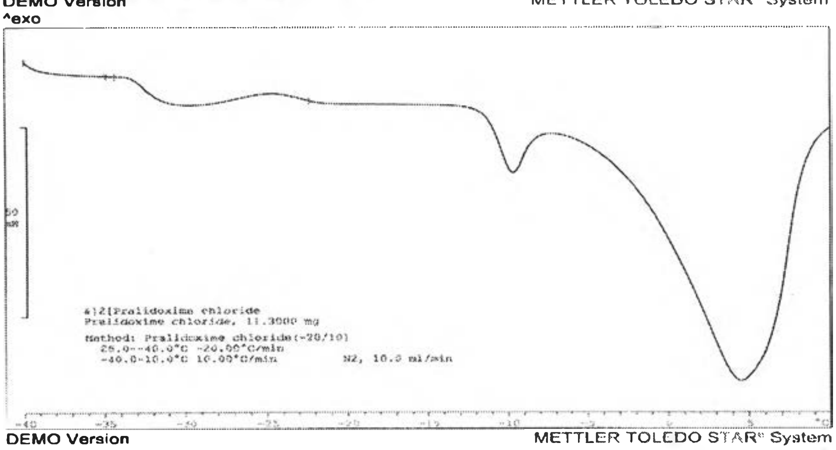

D: Cooling rate = 20°C/min.

Figure 17 DSC thermogram with the same heating rate of 10°C/min but with various cooling rates

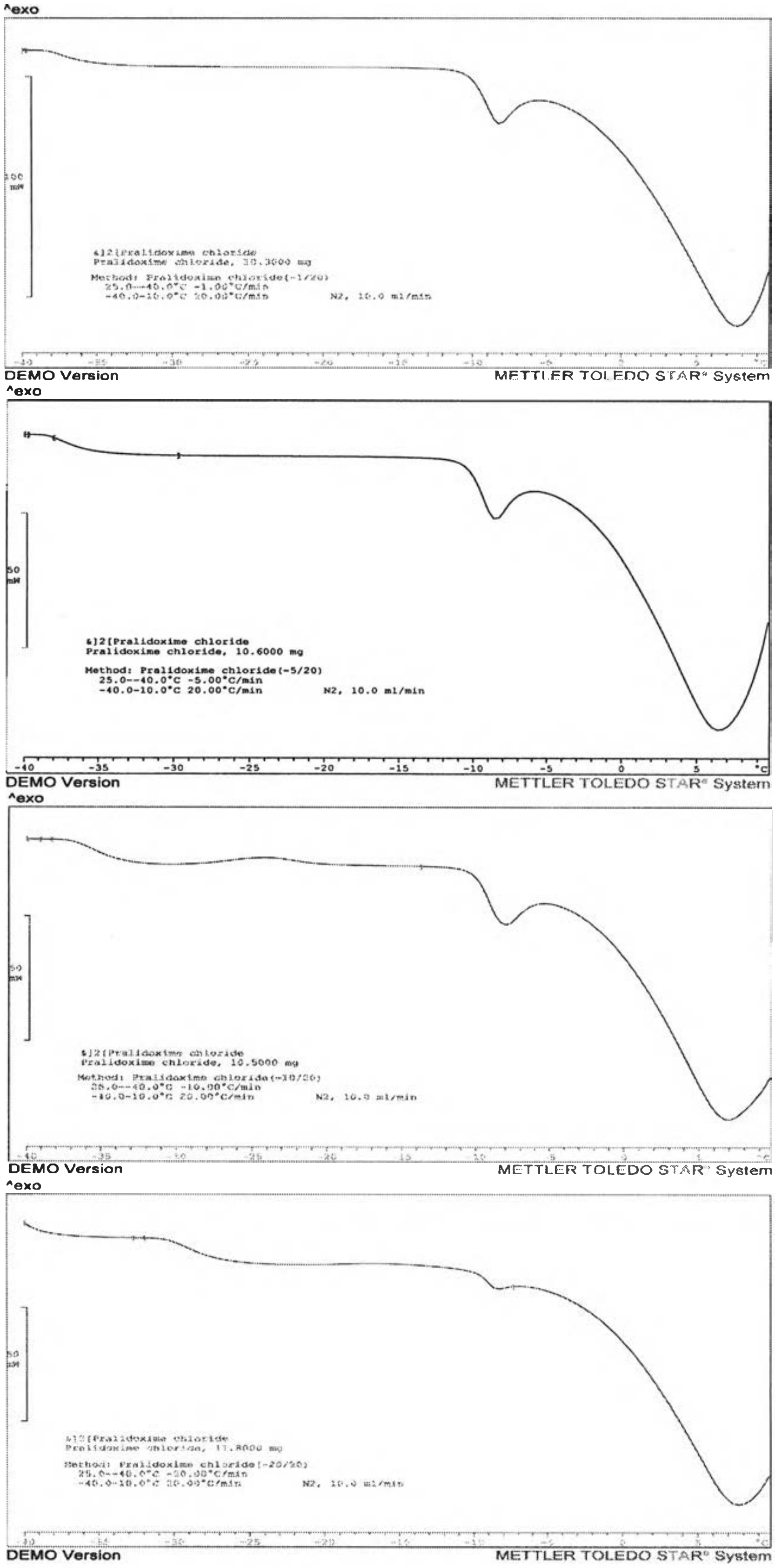

A: Cooling rate = 1°C/min.

B: Cooling rate = 5°C/min.

C: Cooling rate = 10°C/min.

D: Cooling rate = 20°C/min.

Figure 18 DSC thermogram with the same heating rate of 20°C/min but with various cooling rates

In Figure 19, DSC thermograms of pralidoxime chloride solution were scanned by using same cooling rate at 1^{O}C/min but different heating rates of 1, 5, 10 and 20^{O}C/min. The endothermic peaks appeared at different temperature positions. There are three endothermic peaks at the heating rate of 1^{O}C/min. At higher heating rates, the endothermic peaks are showed only two peaks in the thermograms.

For Figures 20, 21 and 22, the cooling rates were set at 5, 10 and 20^{O}C/min, respectively. The DSC patterns appeared in the same way as in Figure 19. The endothermic peaks and the resolution decreased from three to two peaks when the heating rate is faster.

2.2 Thermal behavior with thermal treatment

2.2.1 Annealing before the predetermined freezing temperature.

Samples were cooled from room temperature (25^{O}C) at the rate of 20^{O}C/min to the designated annealing temperatures and annealed at this temperature for 1 hr. The annealing temperatures selected were at -12, -15 and -17^{O}C, where they were situated around the two important sub-zero endotherms obtained from the experiments shown in figure 15D. The DSC thermograms obtained from this experiment (at a heating rate of 1^{O}C/min) are illustrated in Figure 23 for the annealing temperatures of -12, -15 and -17^{O}C.

From experiment 2.2, DSC thermograms without annealing represent the endothermic peaks at approximately -12, -10 and 0^{O}C. In this experiment, the endothermic peaks were at temperatures of -11.4, -9.5 and -2.4^{O}C with respect to all three annealing temperatures used (Figure 23).

2.2.2 Annealing after the predetermined freezing temperature.

Samples were cooled from room temperature (25^{O}C) to the final freezing temperature (-40^{O}C) and then heated (at rate of 1^{O}C/min) to the designated annealing temperatures and annealed at that temperature for 1 hr. In this study, the designated annealing temperatures were also set at -12, -15 and -17^{O}C as in experiment 2.3.1. The samples were then heated from the annealed temperatures to 10^{O}C at the rate of 1^{O}C/min. The DSC thermograms are shown in Figure 24 for the annealing temperatures of -12, -15 and -17^{O}C.

From Figure 24, the endothermic peaks appeared at temperatures of approximately -11.3, -9.5 and -2.6^{O}C when annealing temperature -12 and -15^{O}C were used. The endothermic peaks of the thermogram at annealing temperature of -17^{O}C are -12.2, -10.3 and -3.2^{O}C.

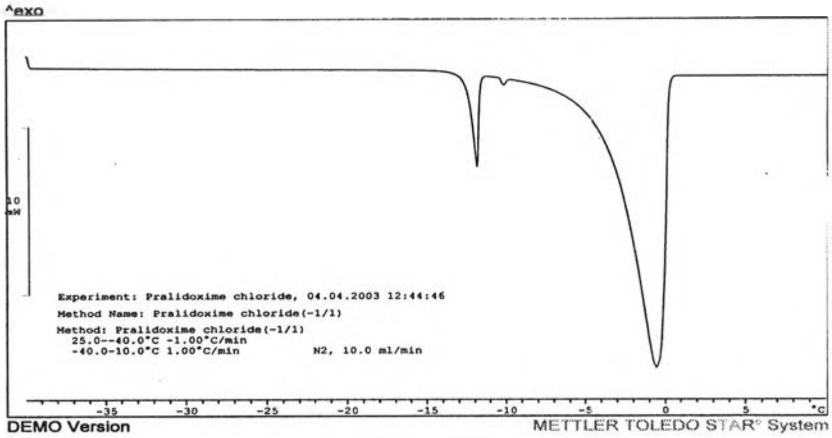

A: Heating rate = 1°C/min.

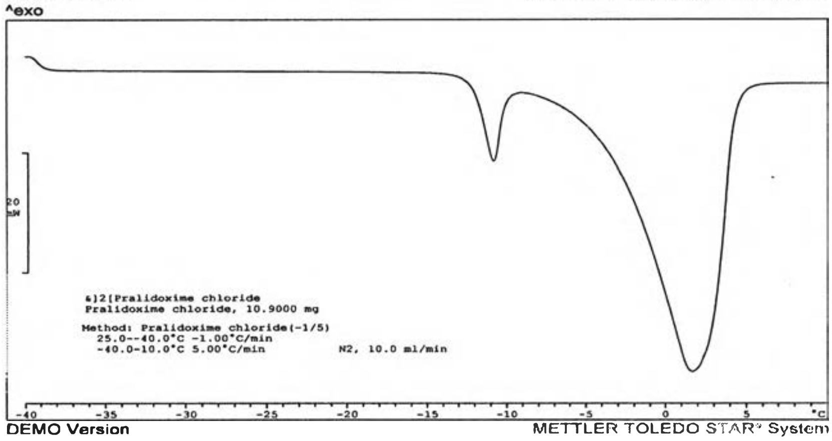

B: Heating rate = 5°C/min.

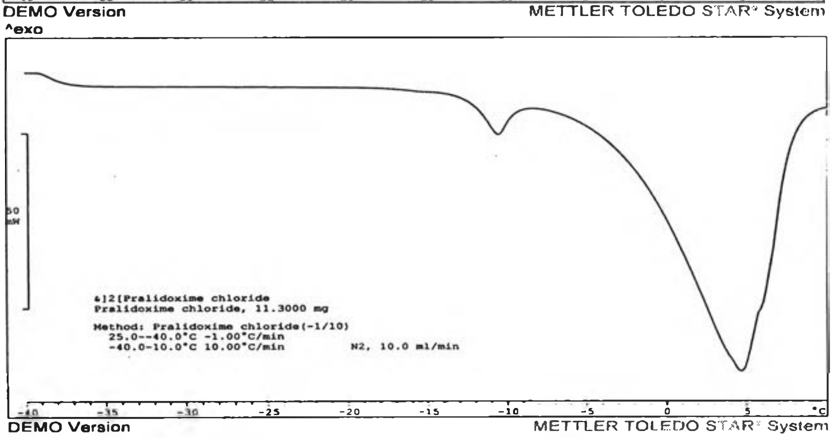

C: Heating rate = 10°C/min.

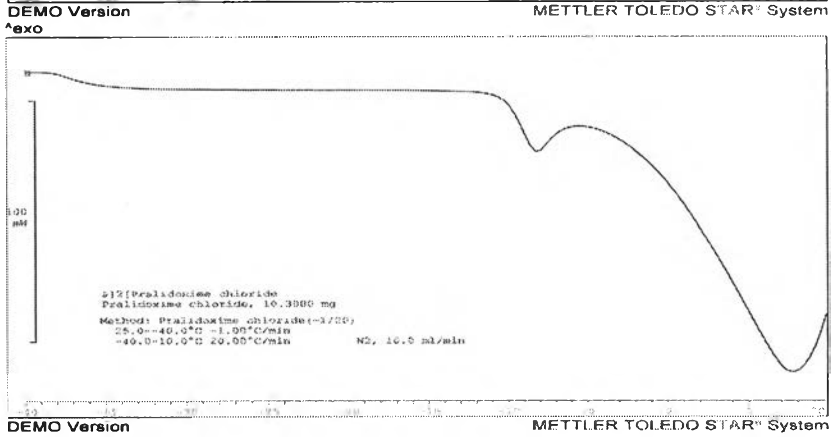

D: Heating rate = 20°C/min.

Figure 19 DSC thermogram with the same cooling rate of 1°C/min but with various heating rates.

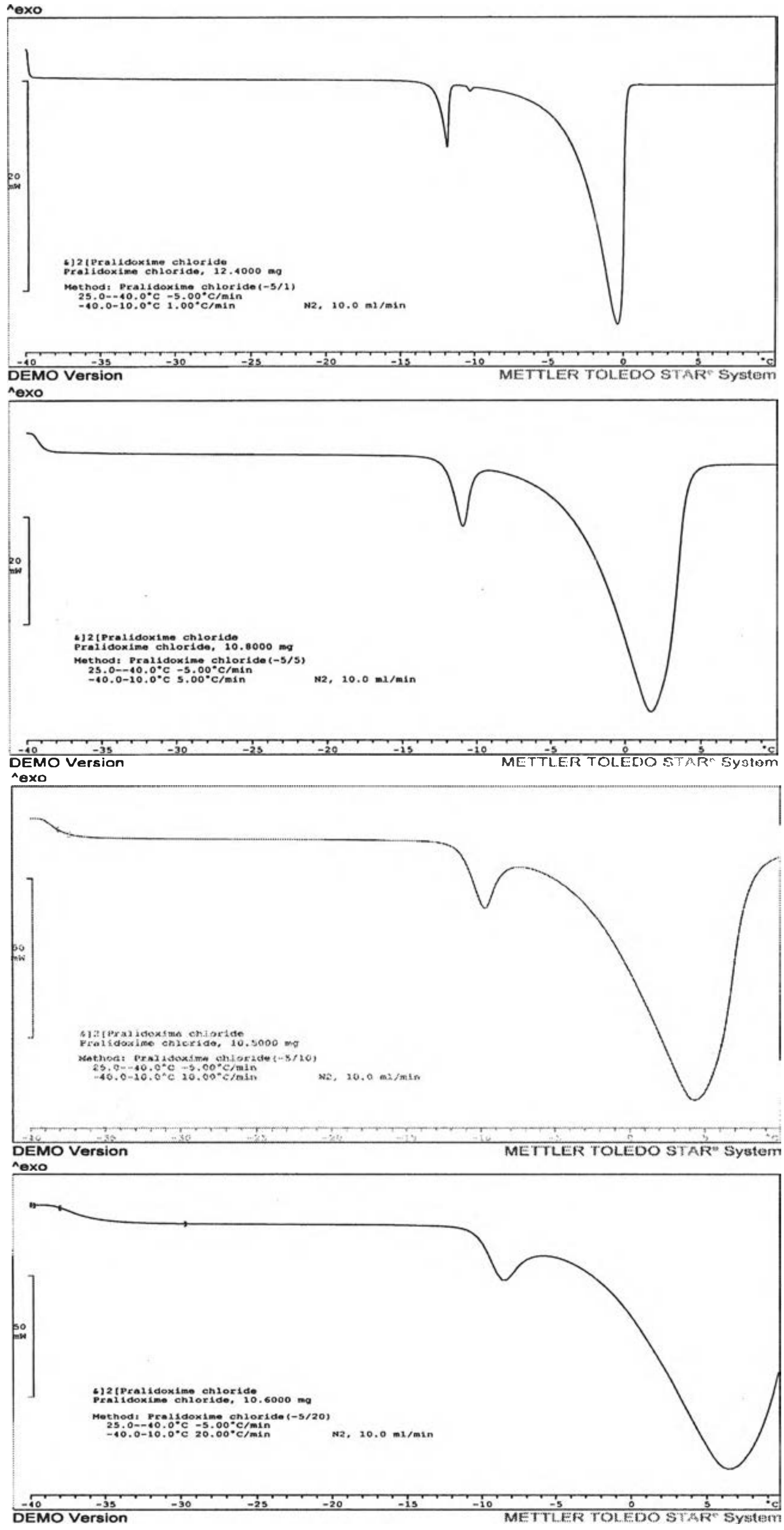

A: Heating rate = 1°C/min.

B: Heating rate = 5°C/min.

C: Heating rate = 10°C/min.

D: Heating rate = 20°C/min.

Figure 20 DSC thermogram with the same cooling rate of 5°C/min but with various heating rates.

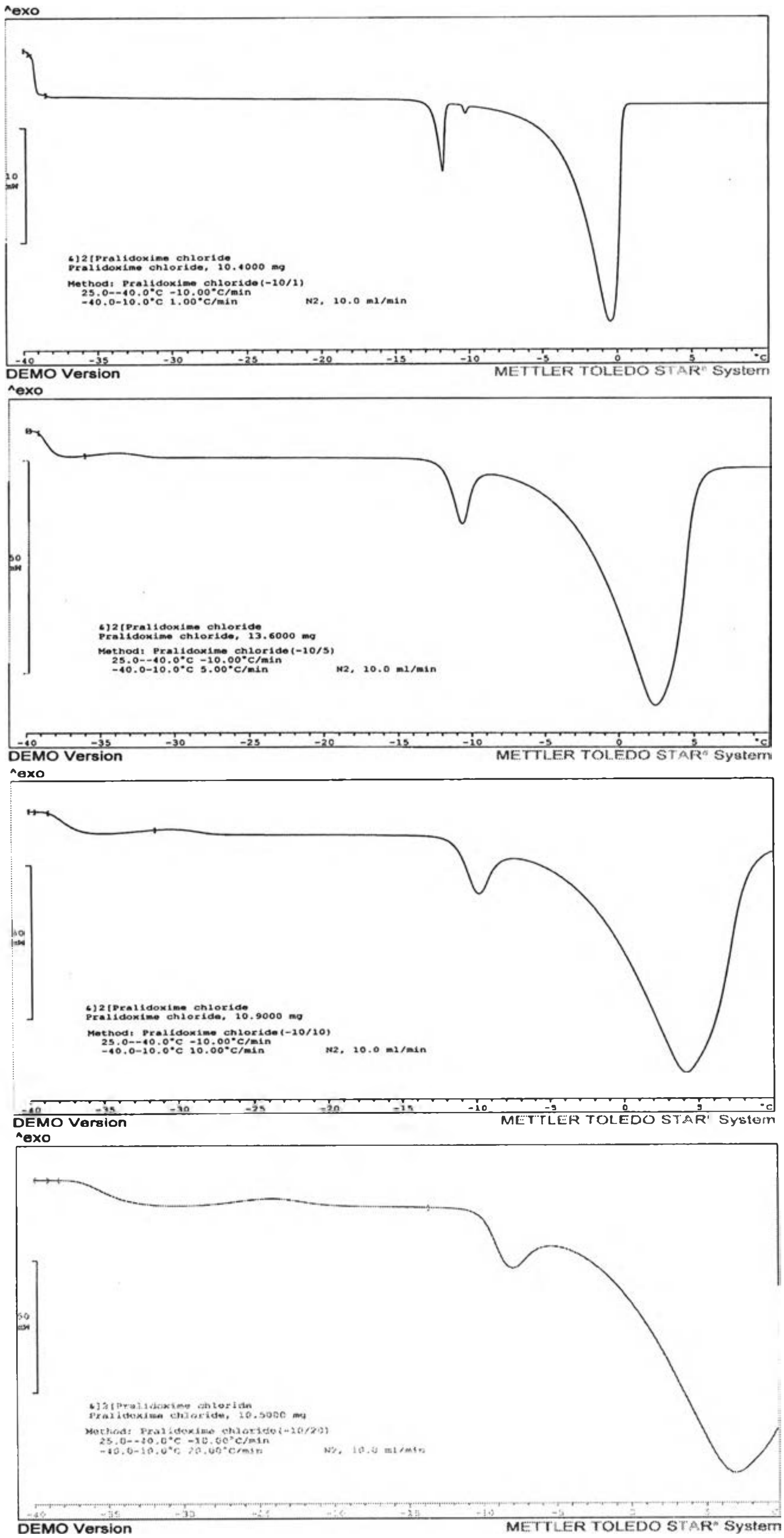

A: Heating rate = 1°C/min.

B: Heating rate = 5°C/min.

C: Heating rate = 10°C/min.

D: Heating rate = 20°C/min.

Figure 21 DSC thermogram with the same cooling rate of 10°C/min but with various heating rates.

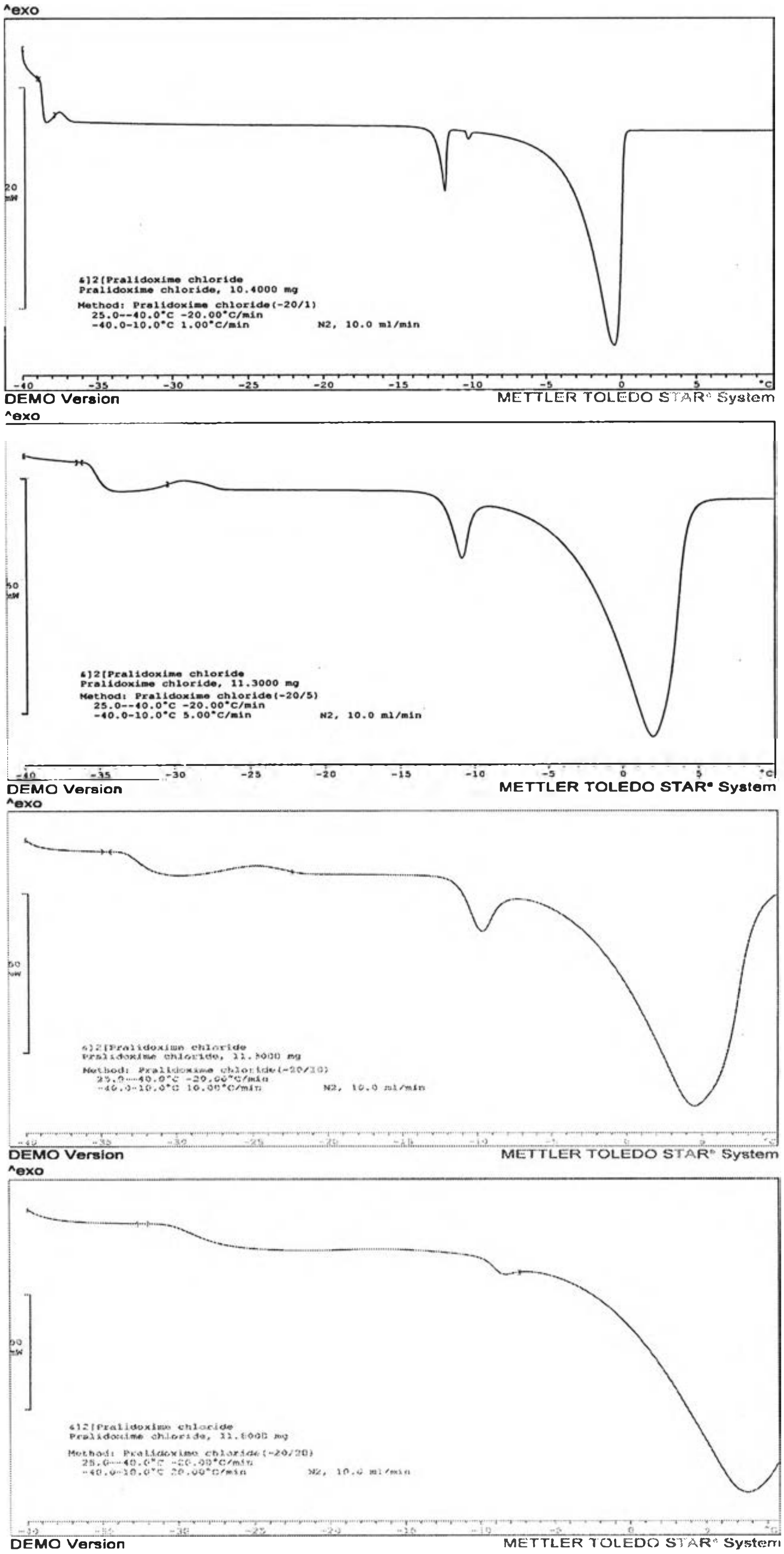

A: Heating rate = 1°C/min.

B: Heating rate = 5°C/min.

C: Heating rate = 10°C/min.

D: Heating rate = 20°C/min.

Figure 22 DSC thermogram with the same cooling rate of 20°C/min but with various heating rates.

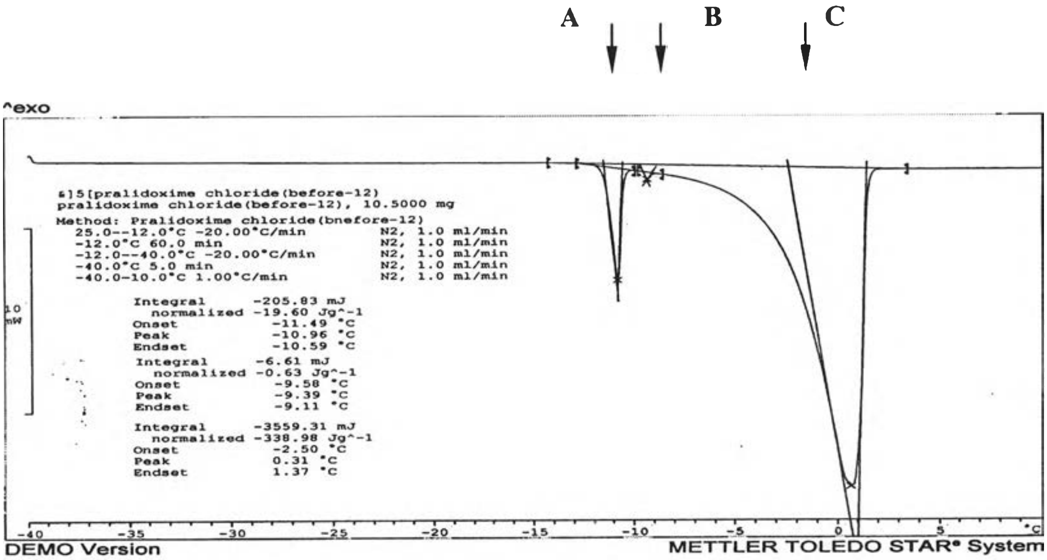

A: 12°C

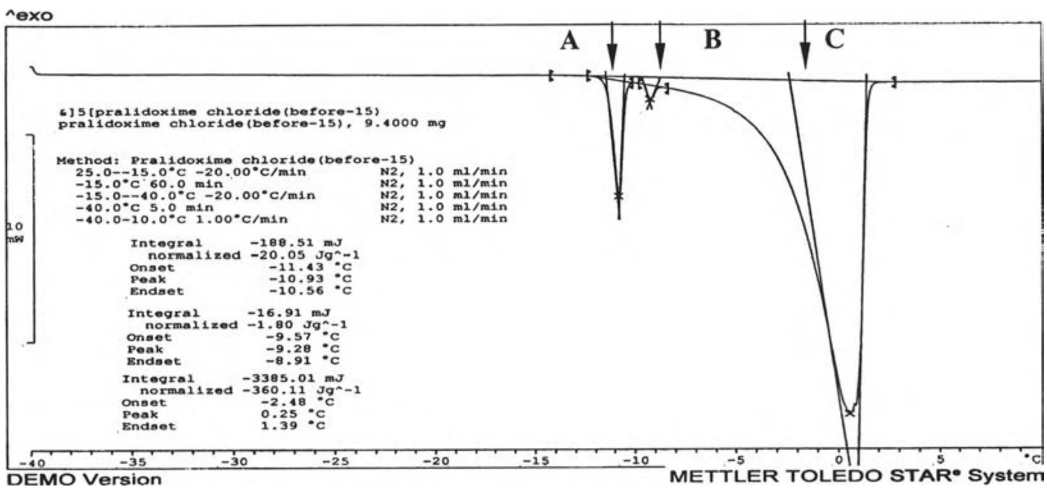

B: -15°C

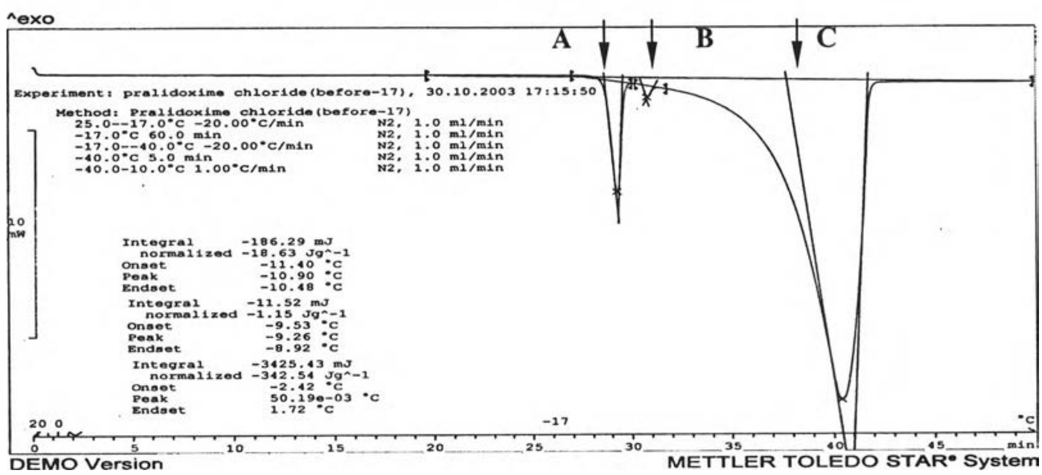

C: -17°C

Figure 23 DSC thermogram: Annealing temperatures of -12, -15 and -17°C for 1 hr **before** the predetermined freezing temperature. (Cooling rate = 20°C/min, Heating rate = 1°C/min)

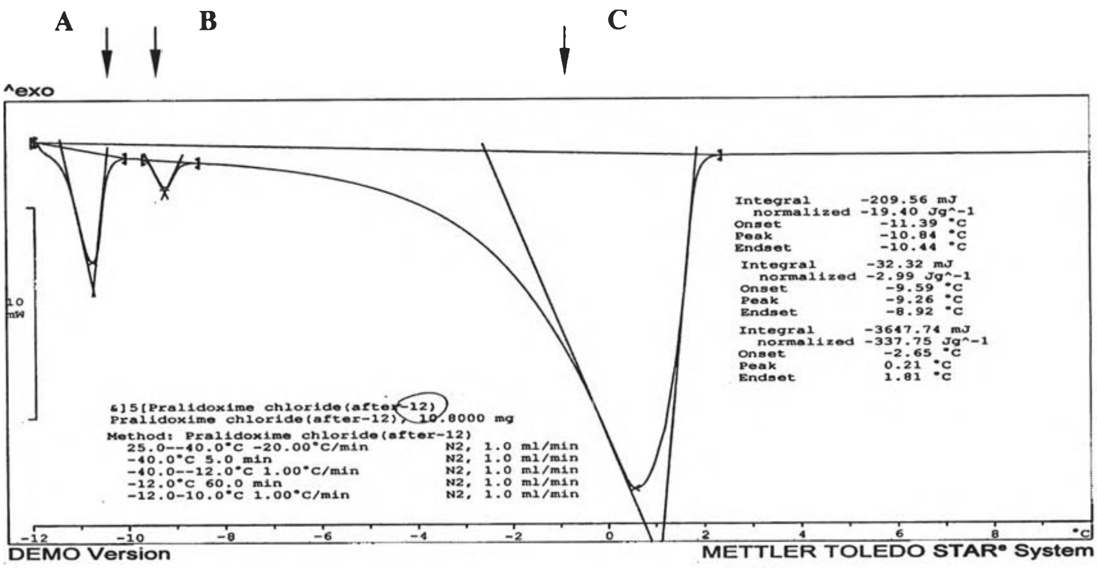

A: -12°C

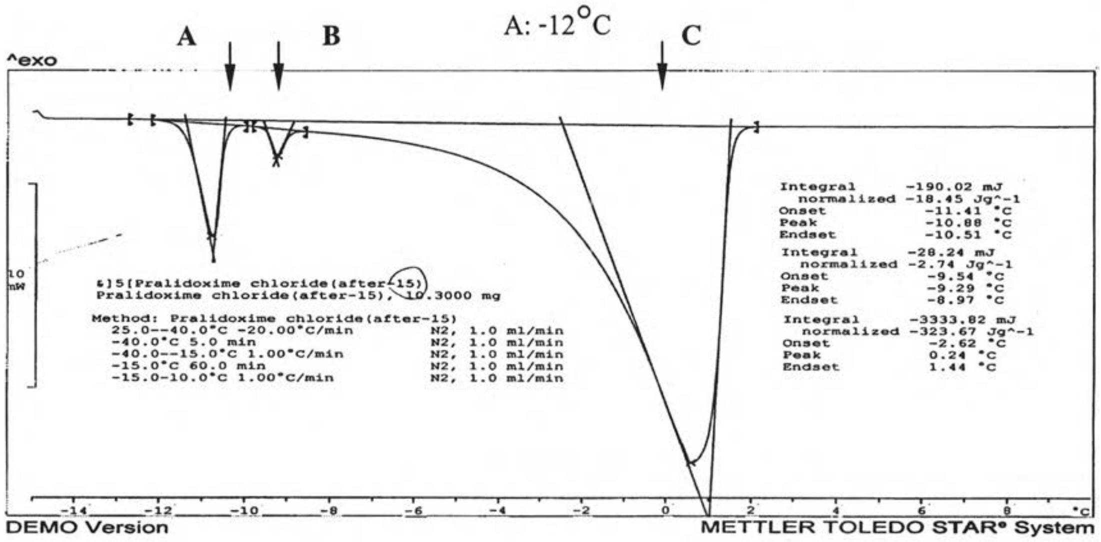

B: -15°C

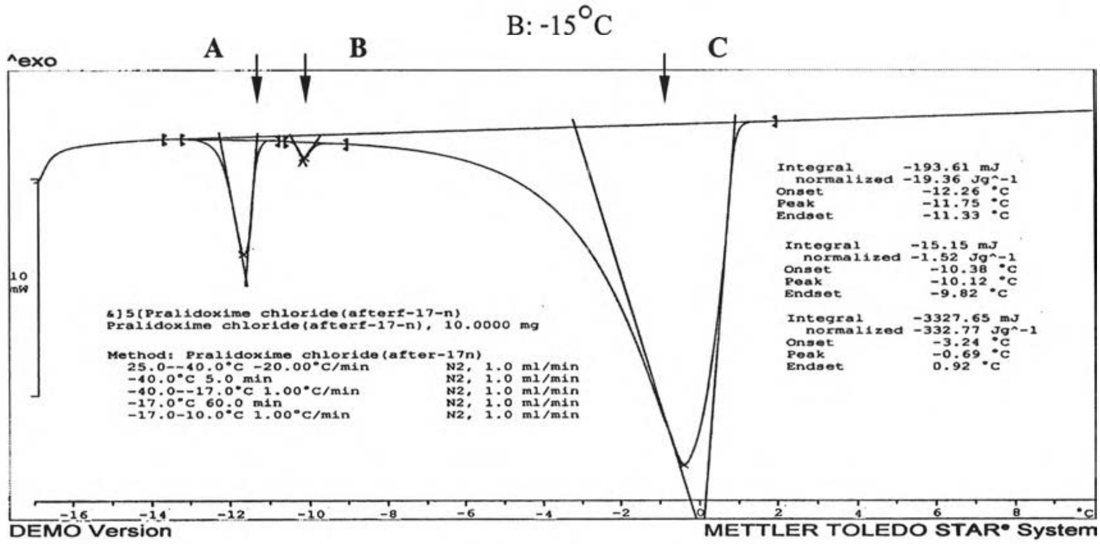

C: -17°C

Figure 24 DSC thermogram: Annealing temperatures of -12, -15 and -17°C for 1 hr **after** the predetermined freezing temperature. (Cooling rate = 20°C/min, Heating rate = 1°C/min)

3 Freeze drying experiment

The 5% sample solutions were subjected to freeze drying cycle using freezing temperature rates and annealing temperatures reminiscent to the DSC freezing condition obtained from 2.2.1 and 2.2.2 to hopefully produce the desired solid structure.

3.1 Annealing before the predetermined freezing temperature

The photographs of pralidoxime chloride freeze dried products are shown in Figure 25. The appearance of freeze dried pralidoxime chloride products were well-formed cakes with the dried solid with the same volume as the solution prior to freeze drying. The colors of all products were also white. The freeze dried products composed of fine powder network in the compact cake and did not separate when the vial was turned up side down.

3.2 Annealing after the predetermined freezing temperature

The photographs of pralidoxime chloride freeze dried products are shown in Figure 26. The appearance of freeze dried products are well-formed cakes but was separated from the vial when turned over. The color was also white. The freeze dried products composed of loosely aggregated crystal and consisted of many pores.

4 Characterization of freeze dried pralidoxime chloride

The freeze dried pralidoxime chloride was subjected to the following analytical procedures.

4.1 X-Ray Powder Diffractometry (XRPD)

The representative powder x-ray diffraction patterns for freeze dried pralidoxime chloride annealed at -12, -15 and -17°C before reaching final freezing temperature are depicted in Figure 27. The important peaks were sharp and intense at 17° and 28$^{\circ}2\theta$.

The X-ray diffraction pattern for freeze dried pralidoxime chloride annealed after reaching freezing temperature at -12,-15 and -17°C are depicted in Figure 28. The intensity of the high crystallinity peaks at 17° and 28° still remained.

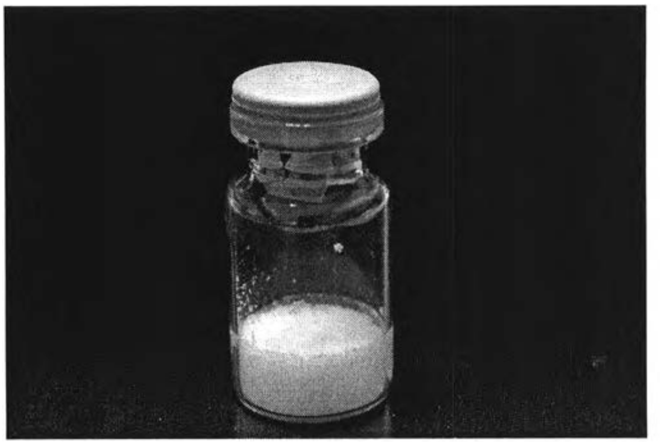

Annealed at -12°C

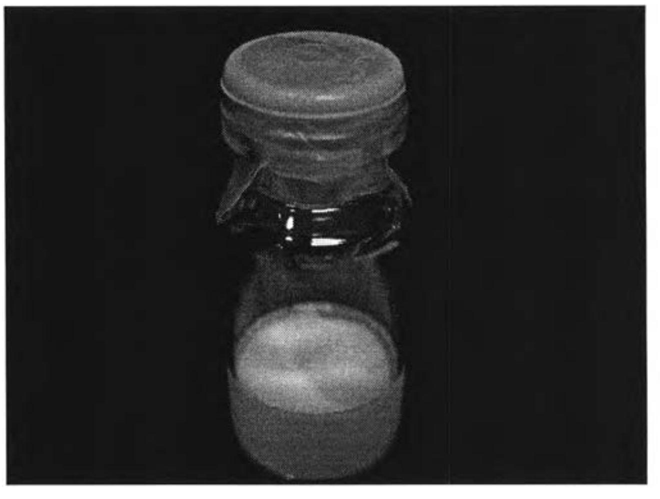

Annealed at -15°C

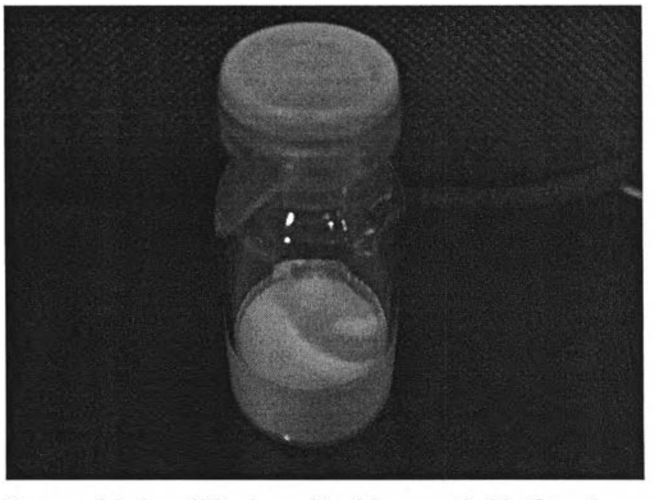

Annealed at -17°C

Figure 25 Freeze dried pralidoxime chloride annealed before the predetermined freezing temperature

Annealed at -12°C

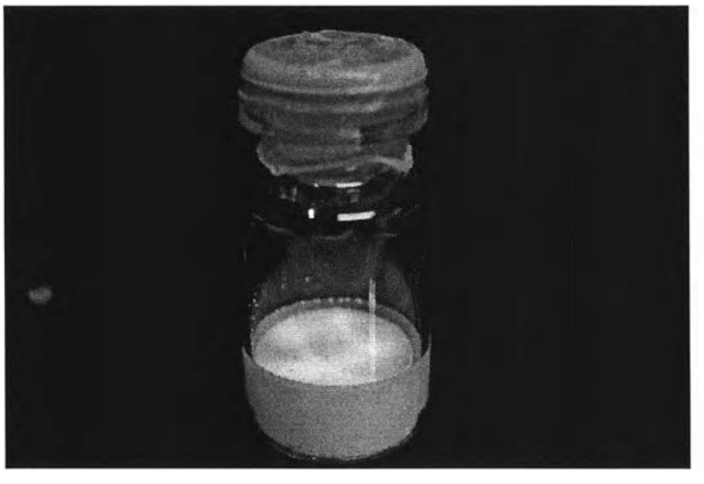

Annealed at -15°C

Annealed at -17°C

Figure 26 Freeze dried pralidoxime chloride annealed after the predetermined freezing temperature

4.2 Scanning Electron Microscopy (SEM)

The photomicrographs of freeze dried pralidoxime chloride, annealed before the predetermined freezing temperature, are shown in Figure 29-31. The SEM photomicrographs indicate irregular shape of crystals with smooth surface. The morphology of freeze dried pralidoxime chloride for the three annealing conditions looked similar. The crystal flakes were observed and the surface of freeze dried products were porous similar to that of a bone structure.

The SEM photomicrograph of freeze dried pralidoxime chloride annealed after the predetermined freezing temperature is shown in Figures 32, 33 and 34, respectively.

4.3 Thermal analysis study

Freeze dried pralidoxime chloride was scanned at the rate of 10°C/min from 25°C to 300°C. DSC thermograms are represented in Figures 35 for the freeze dried solids obtained by annealing prior to freezing. Also, Figures 36 are thermograms of freeze dried solids obtained by annealing after freezing at different annealing temperature..

The DSC thermogram represented the melting point of freeze dried products from annealing before condition at approximately around 225°C. The thermograms obtained with samples annealed after reaching final freezing temperature showed that the melting point is located around 230°C.

5. Stability of freeze dried pralidoxime chloride

The solid state stability of freeze dried pralidoxime chloride was observed under the humid condition and dry condition. The humidity was set at 70% relative humidity by using saturated potassium iodide solution and controlled temperature at 40°C. Samples were chosen for x-ray powder diffraction analysis and photographs of each vial were captured day by day. In this experiment, the freeze dried product used was the one that annealed after reaching the final freezing temperature because of the high amorphous content of this product which made it very unstable.

The pictures of freeze dried pralidoxime chloride from day one to day five under dry condition are shown in Figure 37 and under humid condition are shown in Figure 38. At dry condition, all of freeze dried pralidoxime chloride cakes were found to only slightly collapse after five days experiment. The color of the freeze dried product unchanged.

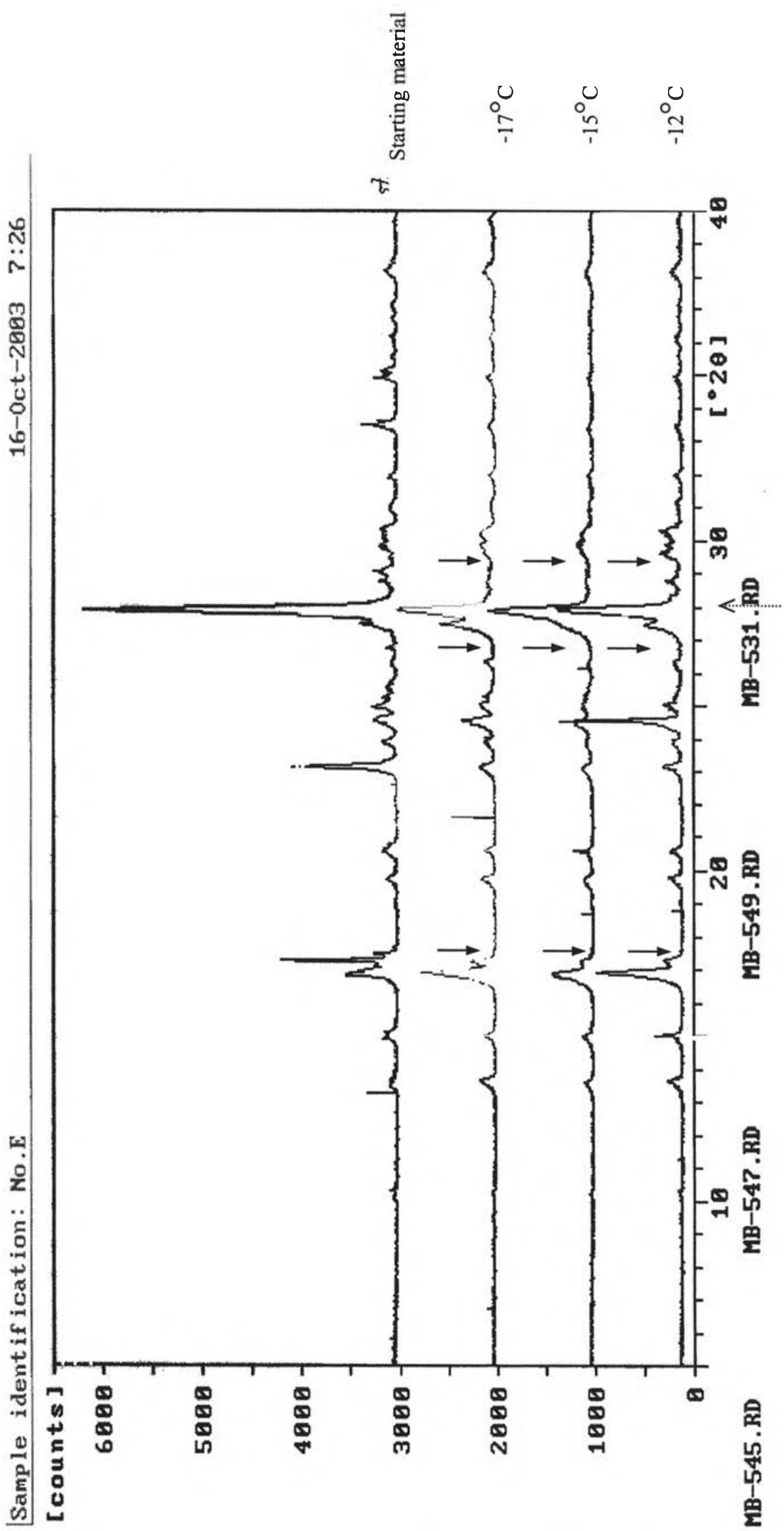

Figure 27 X-ray diffractogram of freeze dried pralidoxime chloride annealed at -12,-15 and -17°C **before** the predetermined freezing temperature compare with pralidoxime chloride starting material

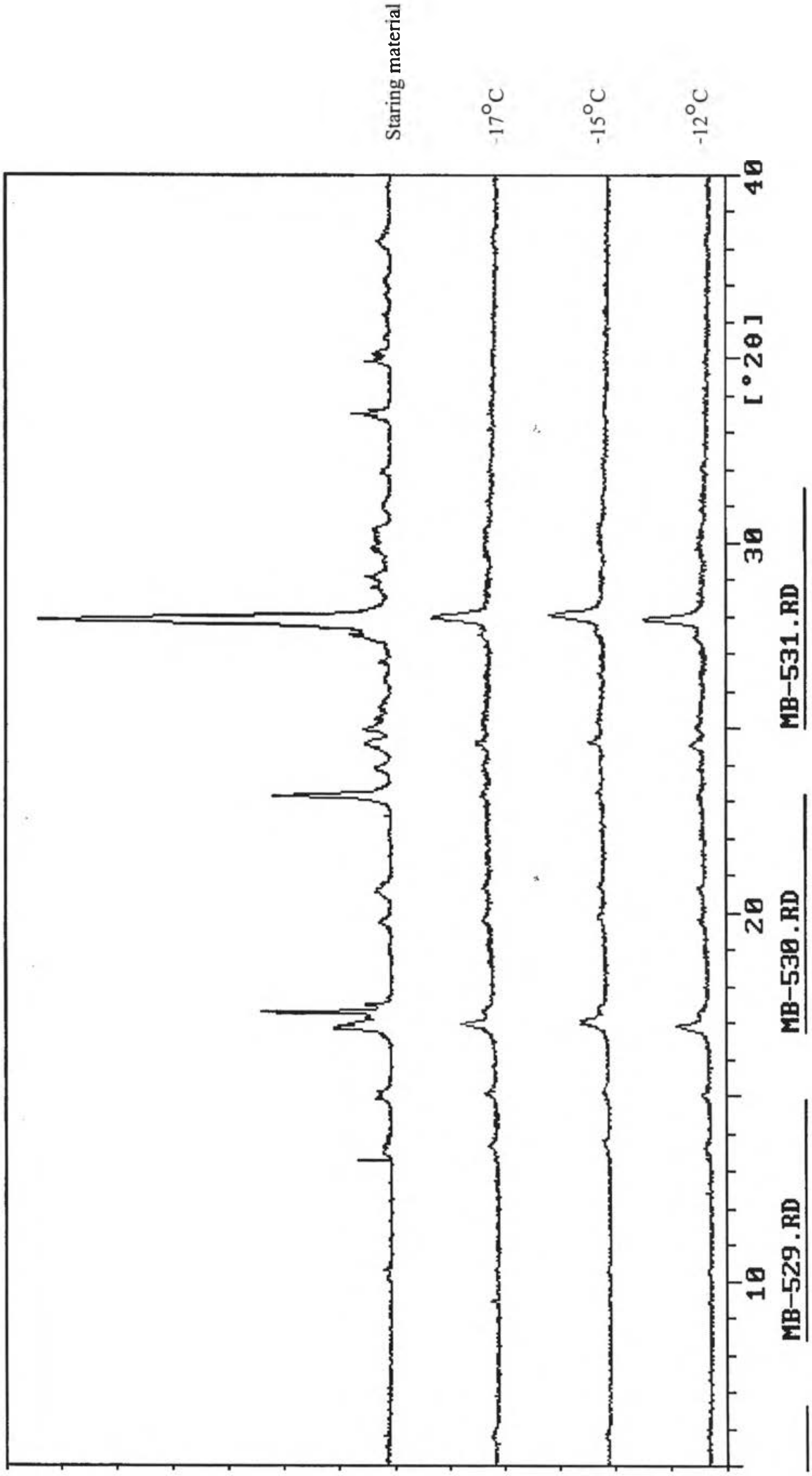

Figure 28 X-ray diffractogram of freeze dried pralidoxime chloride annealed at -12,-15 and -17°C **after** the predetermined freezing temperature compare with pralidoxime chloride starting material

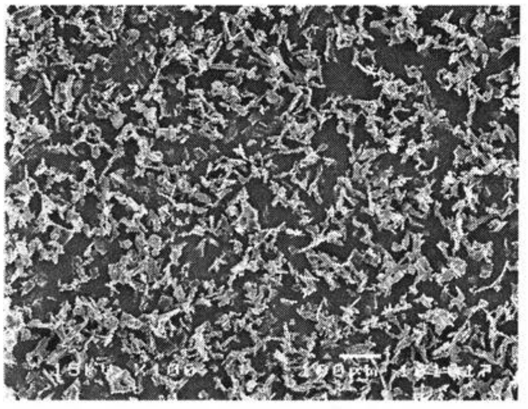

x 100

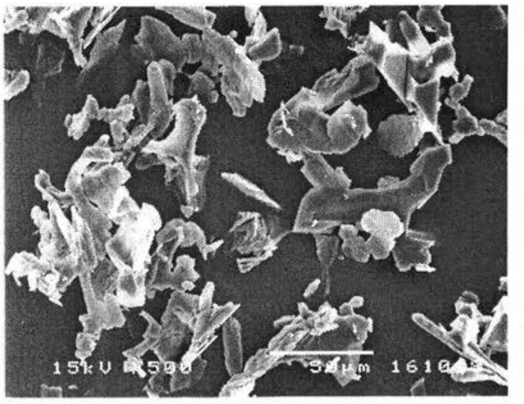

x 500

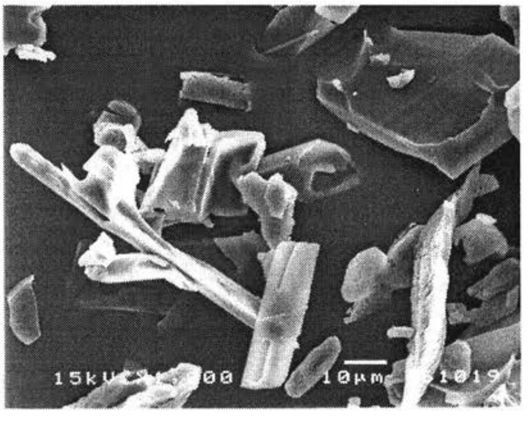

x 1,000

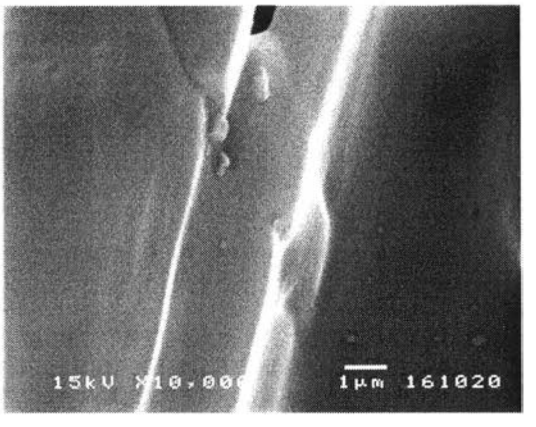

x 10,000

Figure 29 Photomicrograph of freeze dried pralidoxime chloride annealed at -12°C before the predetermined freezing temperature

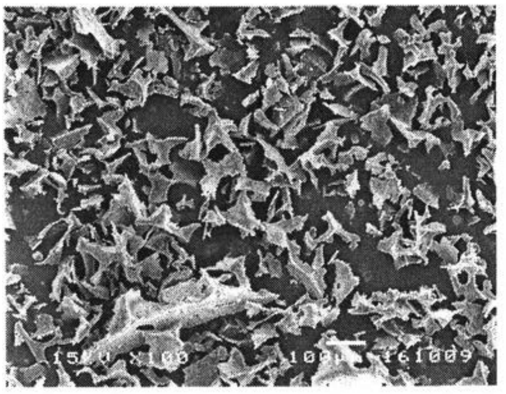

x 100

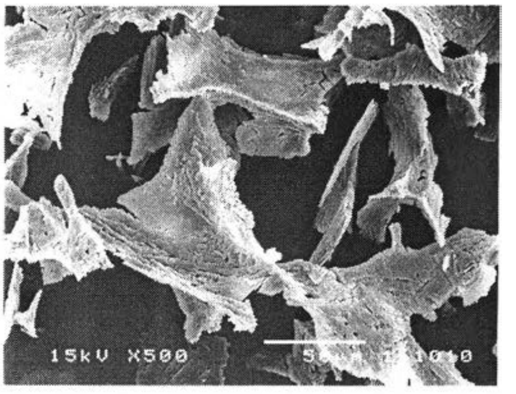

x 500

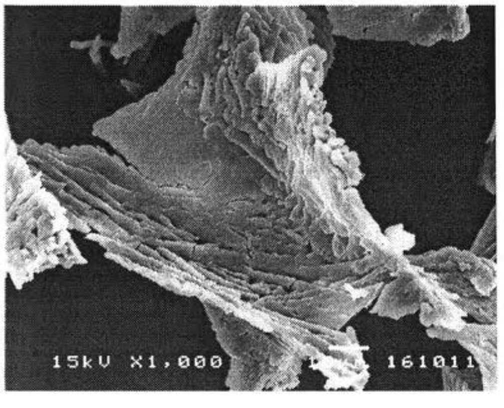

x 1,000

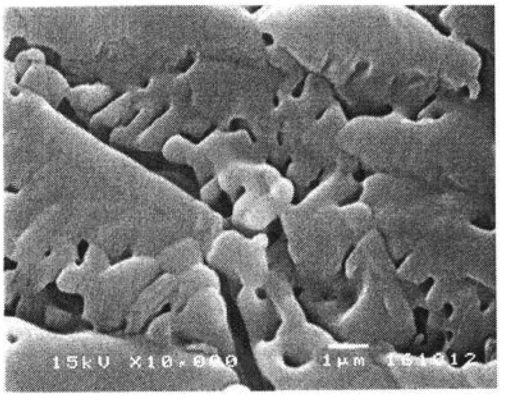

x 10,000

Figure 30 Photomicrograph of freeze dried pralidoxime chloride annealed at -15°C before the predetermined freezing temperature

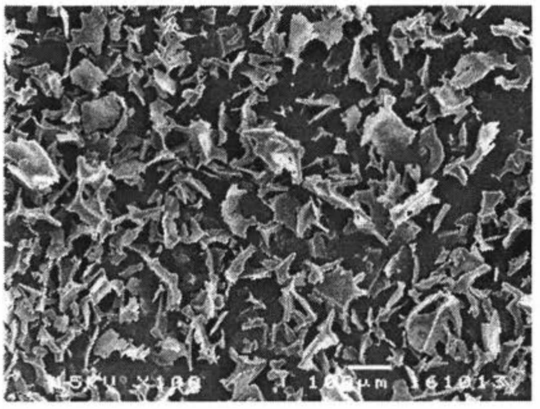

x 100

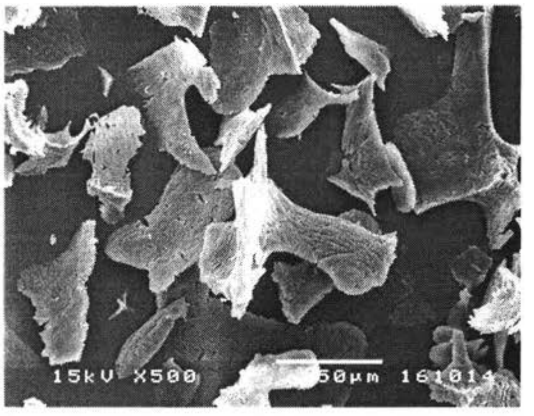

x 500

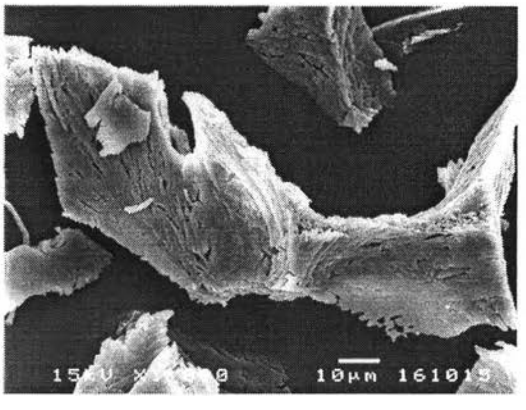

x 1000

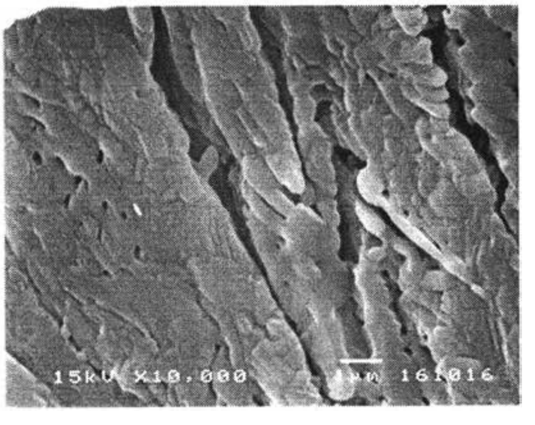

x 10,000

Figure 31 Photomicrograph of freeze dried pralidoxime chloride annealed at -17°C before the predetermined freezing temperature

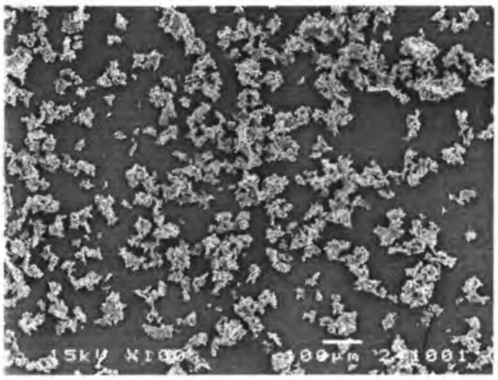

x 100

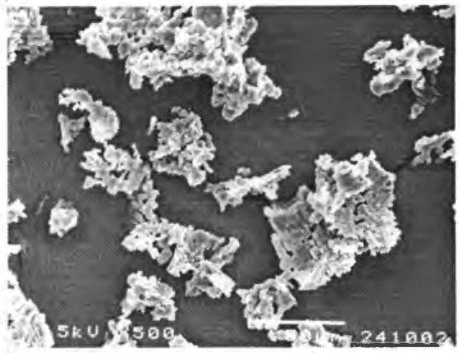

x 500

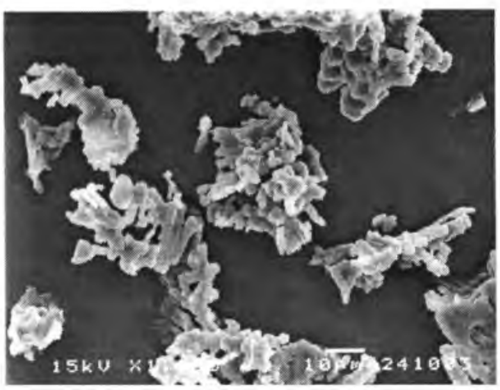

x 1000

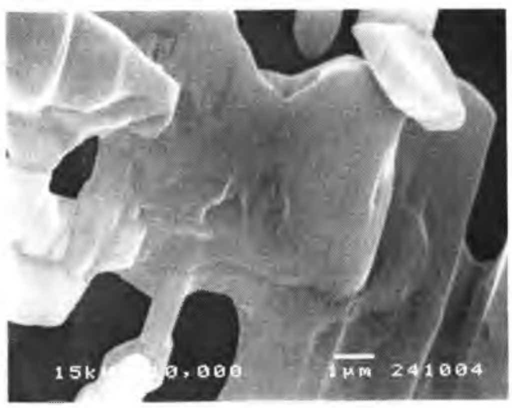

x 10,000

Figure 32 Photomicrograph of freeze dried pralidoxime chloride annealed at -12°C after the predetermined freezing temperature

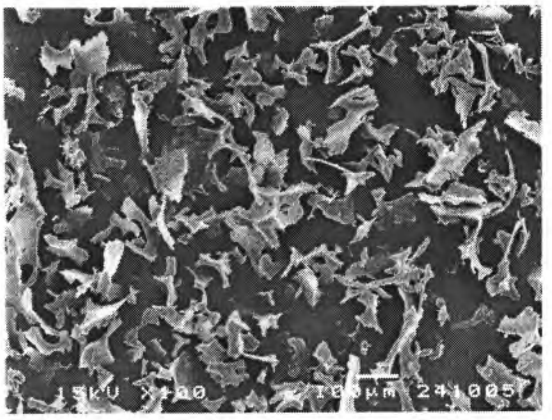

x 100

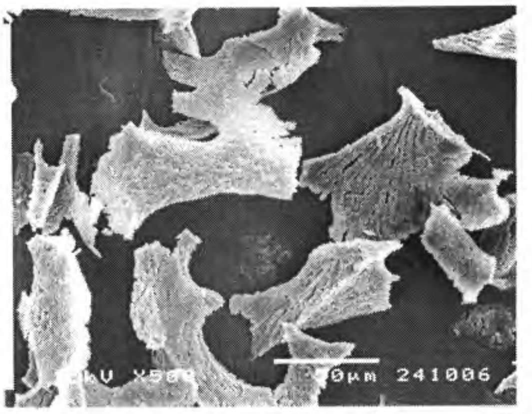

x 500

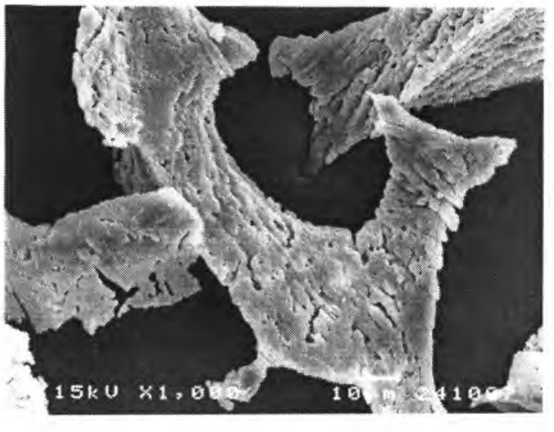

x 1000

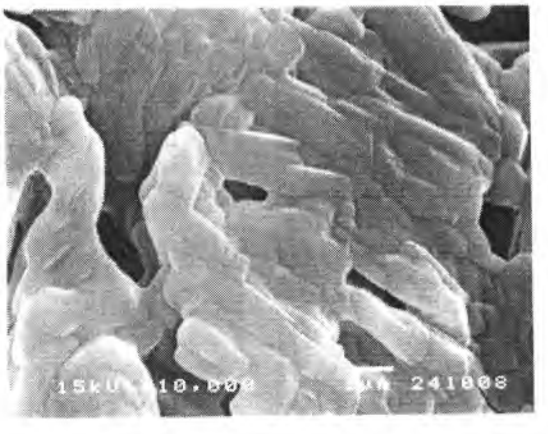

x 10,000

Figure 33 Photomicrograph of freeze dried pralidoxime chloride annealed at -15°C after the predetermined freezing temperature

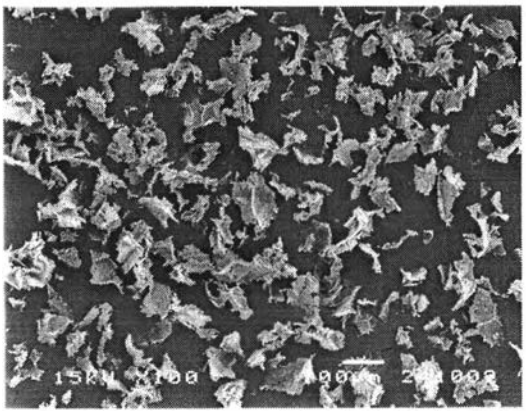

x 100

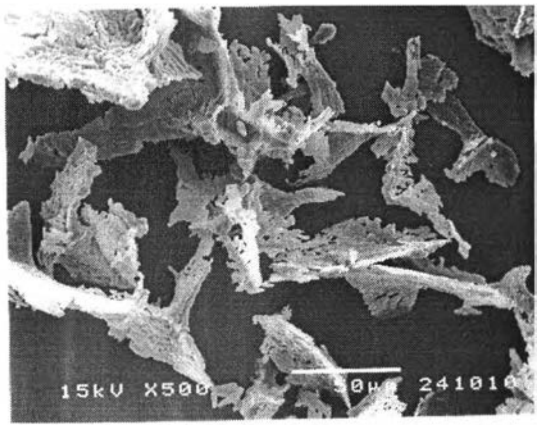

x 500

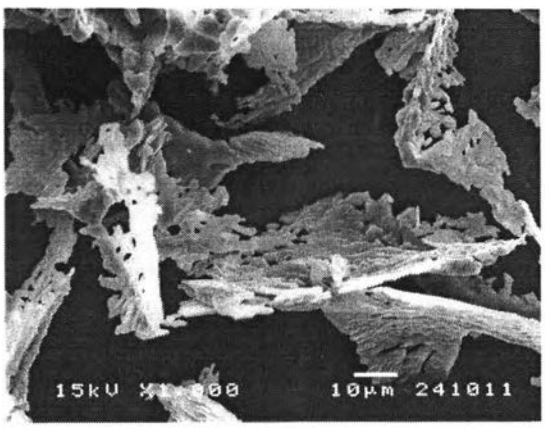

x 1000

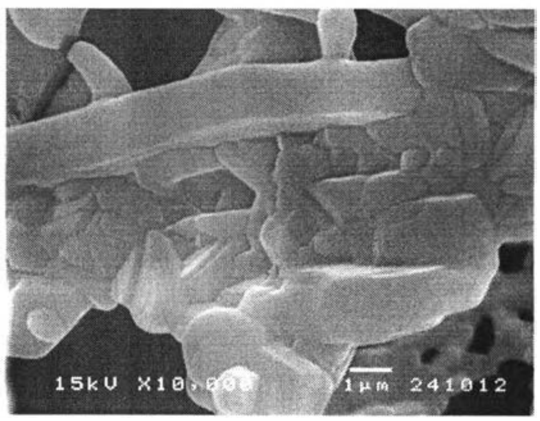

x 10,000

Figure 34 Photomicrograph of freeze dried pralidoxime chloride annealed at -17°C after the predetermined freezing temperature

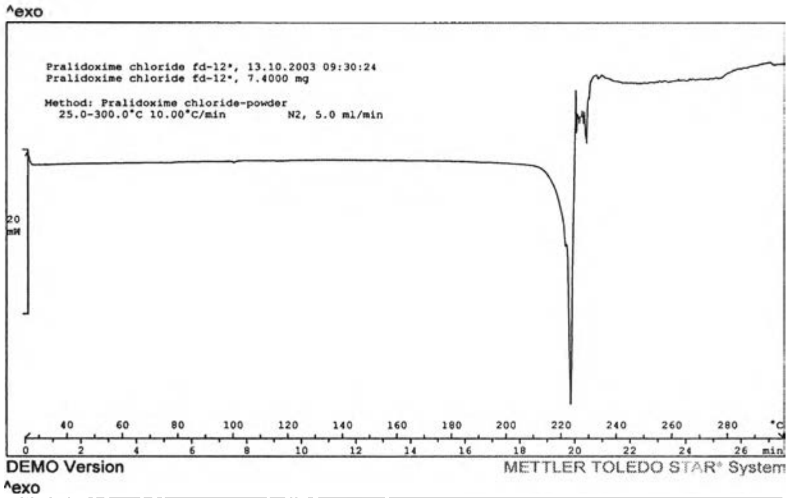

-12°C

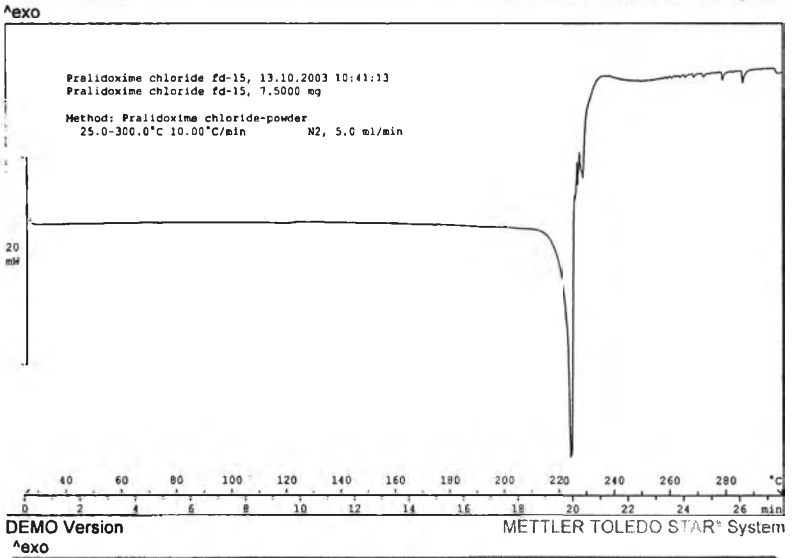

-15°C

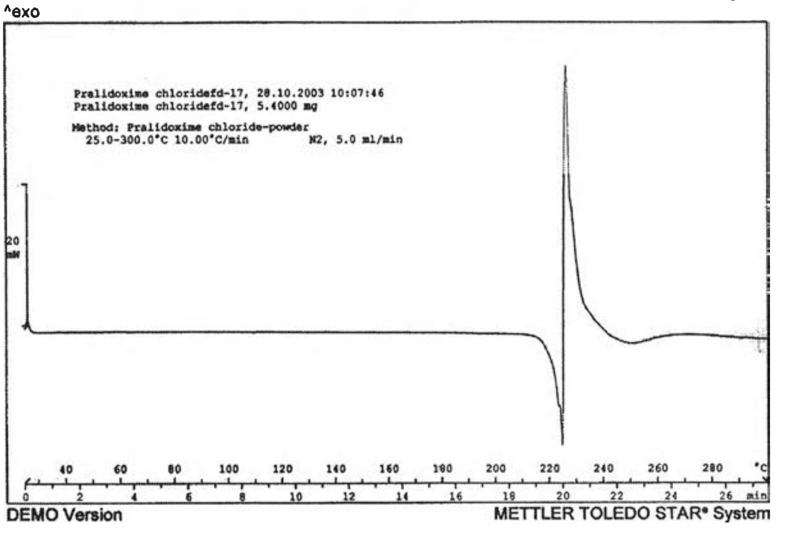

-17°C

Figure 35 DSC thermogram of freeze dried pralidoxime chloride annealed before the predetermined freezing temperature at annealing temperature -12, -15 and -17°C (Scan rate = 10°C/min)

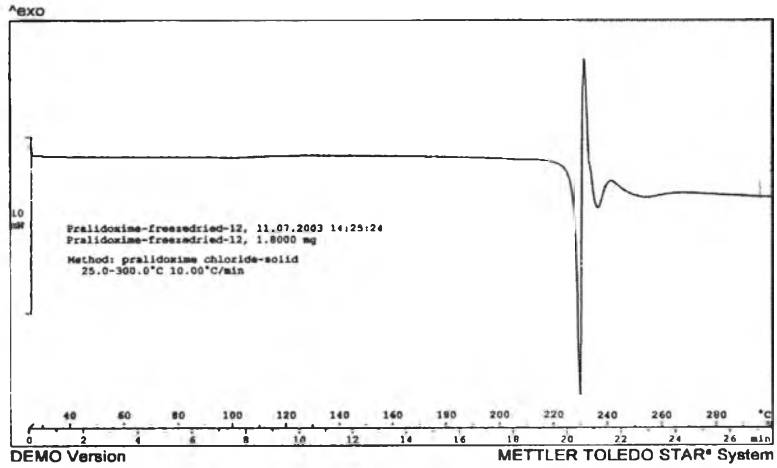

-12°C

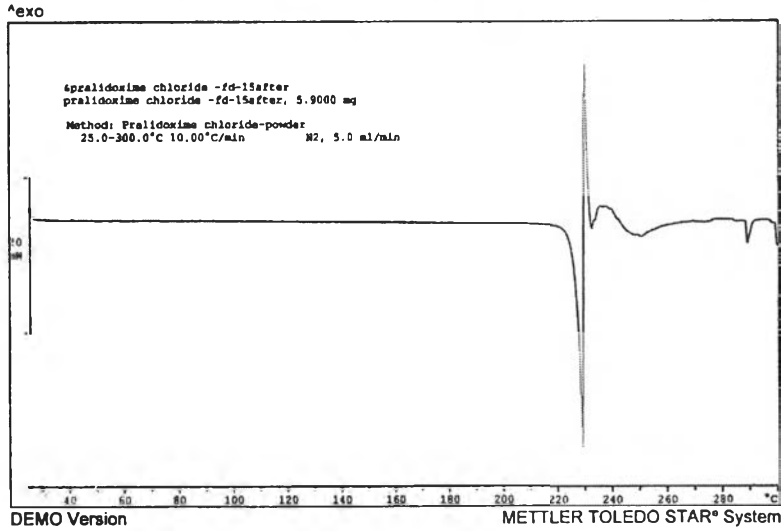

-15°C

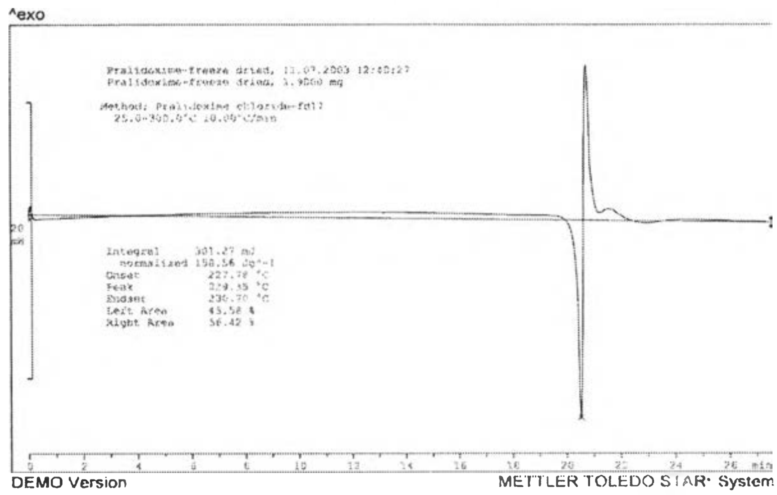

-17°C

Figure 36 DSC thermogram of freeze dried pralidoxime chloride annealed after the predetermined freezing temperature at annealing temperature -12, -15 and -17°C (Scan rate = 10°C/min)

Day 0

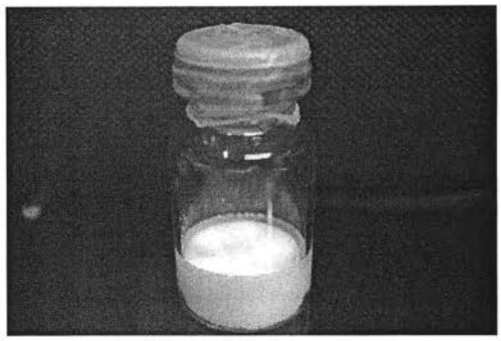

Day 1

Day 2

Day 3

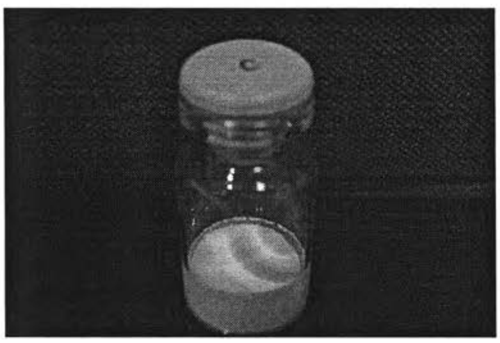

Day 4

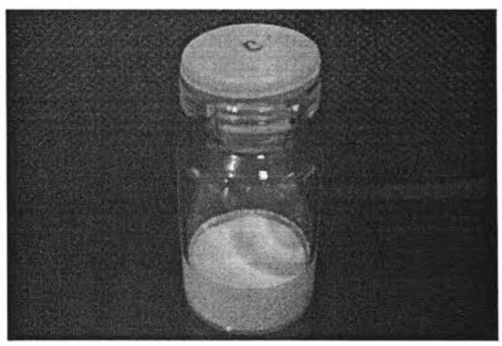

Day 5

Figure 37 The pictures of freeze dried pralidoxime chloride in controlled condition (40°C, 0% RH) from 1-5 days

Day 0

Day 1

Day 2

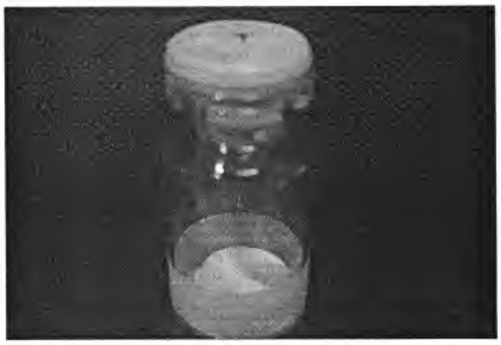

Day 3

Day 4

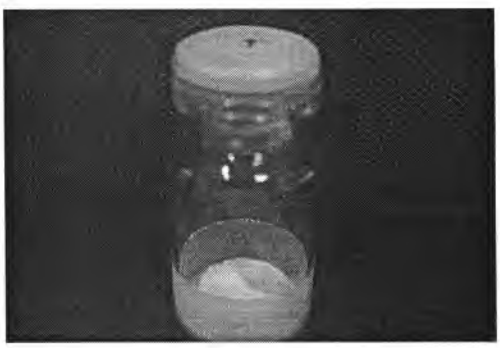

Day 5

Figure 38 The pictures of freeze dried pralidoxime chloride under humid condition ($40^{\circ}C$, 70% RH) from 1-5 days

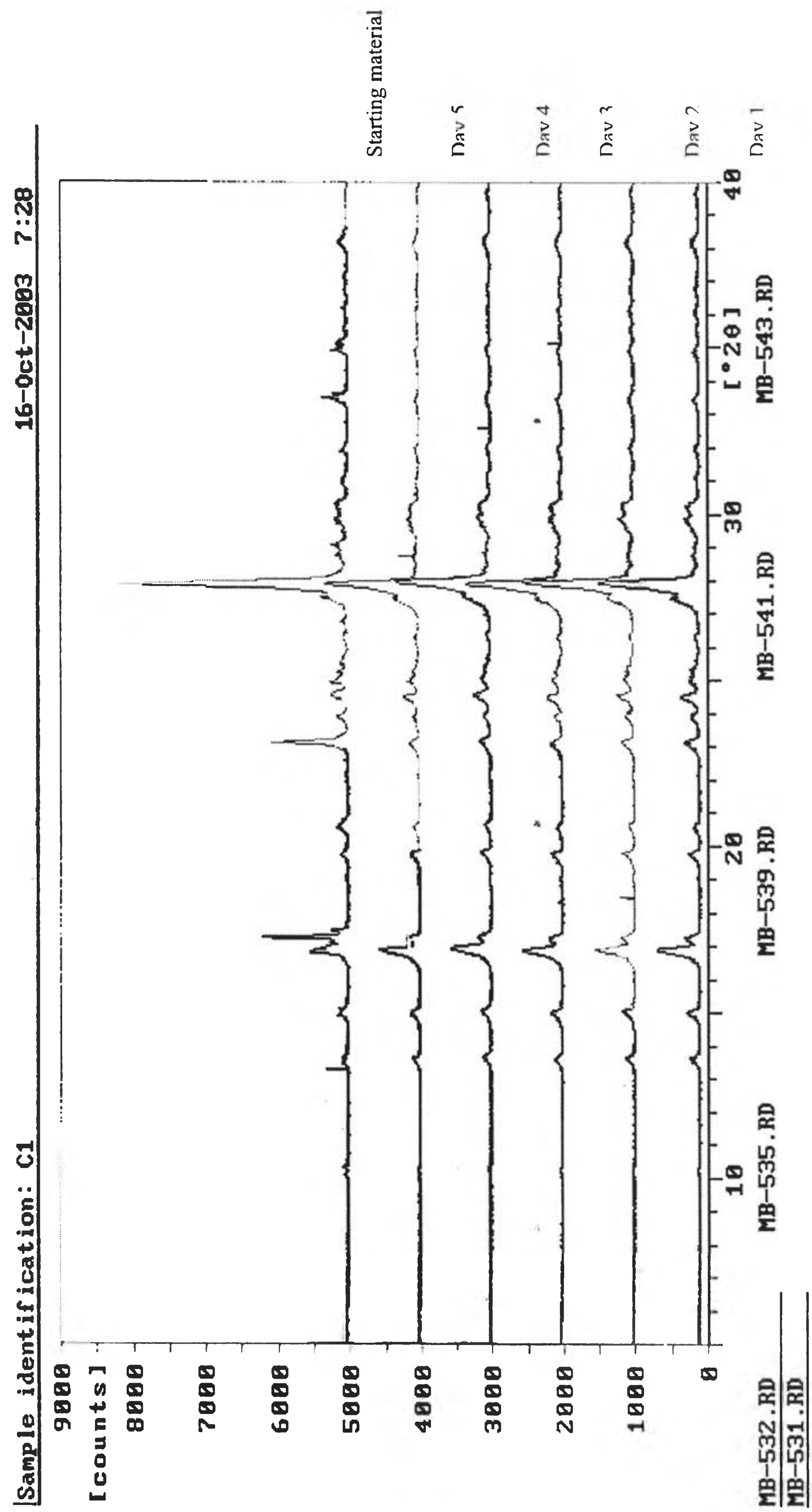

Figure 39 X-ray diffractogram of freeze dried pralidoxime chloride in controlled condition ($40^{\circ}C$, 0% Rh)

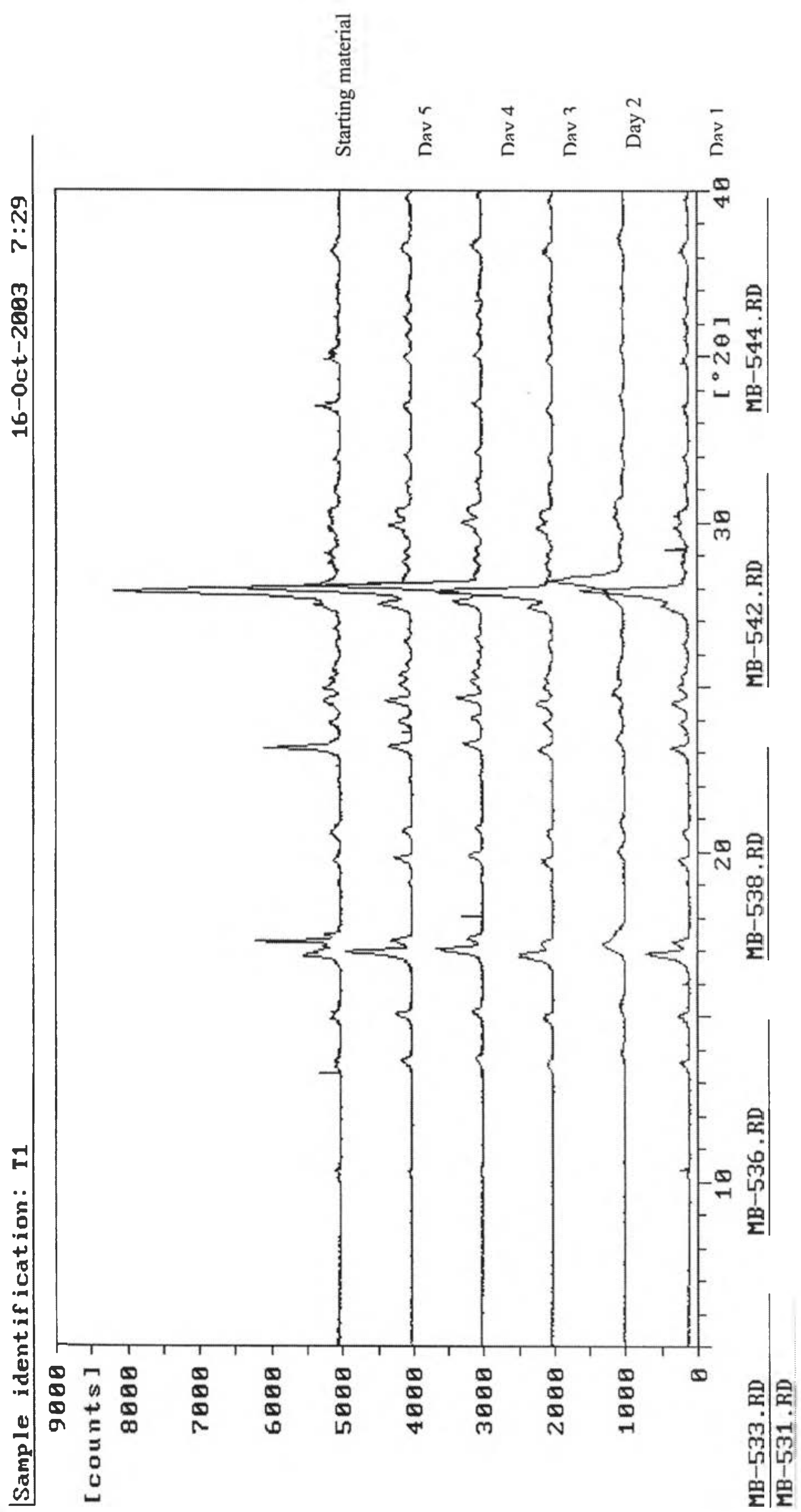

Figure 40 X-ray diffractogram of freeze dried pralidoxime chloride under humid condition ($40^{\circ}C$, 70% Rh)

After exposing to a humid condition, the product was found to shrunk and become collapse after the first day of the experiment. The color of products changed from white to pale yellow. The product looked moist and then wet.